DEVELOPMENT OF A HIGH-TEMPERATURE HIGH-PRESSURE PROCESS FOR THE MANUFACTURE OF DIAMOND-TUNGSTEN-METAL COMPOSITES FOR OIL AND GAS DRILLING

by

Lin Gu

A thesis submitted to the faculty of
The University of Utah
in partial fulfillment of the requirements for the degree of

Master of Science

Department of Metallurgical Engineering

The University of Utah

December 2015

The University of Utah Graduate School

STATEMENT OF THESIS APPROVAL

The thesis of **Lin Gu**

has been approved by the following supervisory committee members:

Zhigang Zak Fang	, Chair	**July 10th, 2015**
		Date Approved
Reaz A. Chaudhuri	, Member	**July 10th, 2015**
		Date Approved
Mark C. Koopman	, Member	**July 10th, 2015**
		Date Approved

and by **Manoranjan Misra** , Chair/Dean of

the Department/College/School of **Metallurgical Engineering**

and by David B. Kieda, Dean of The Graduate School.

ABSTRACT

Diamond-Tungsten-Metal (DTM) matrix composites are a promising material for exploration of the earth's oil and gas, as well as other applications calling for very high abrasion resistance. This material is used for its unique combination of properties, including: abrasive cutting capability, flexural strength, fracture toughness, impact resistance, hardness, and wear resistance. The present work centered on the development of a process for producing this composite material.

A pellet-making process was developed to fabricate DTM particles which could then be directly used for making DTM inserts. Diamond grit was coated with dry, premixed matrix powders (tungsten carbide, cobalt and/or copper) by using sprayed binder liquid and a vibratory machine. This process successfully solved the problem of achieving uniform diamond distribution.

Subsequently, a modified rapid-heating omnidirectional compaction (mROC) process was employed to fully consolidate the the DTM inserts. After DTM pellets were cold pressed under a pressure of 243.71 MPa to create green parts, these samples were then transferred to the hot press machine to undergo the mROC process. The mROC process was initiated by a preheating step at 200-300 °C for debinding for 30 minutes., and then five minutes at elevated temperature to melt the glass by surpassing its melting

temperature. After that, a high temperature (approximately 1200 °C), high pressure (560 MPa) compaction step was operated for another five minutes. Cooling and pressure releasing is the final step, then the DTM inserts were obtained. The process was shown to create matrices with uniform microstructure, although tiny holes caused by free carbon and vaporized wax could still be observed.

In this study, other characteristics and variables with potential effects on mechanical properties and the microstructures of DTM composites were investigated, including diamond-volume percentage and compositional variation of matrices. It was found that both higher diamond-volume percentage (diamond being the primary abrasion particles) and larger tungsten carbide (WC)-content (hard phase and the skeleton of matrix) contributed to the higher hardness of the matrix. In terms of matrix composition, copper was added to the binder phase and was also seen to decrease the average hardness of the composite. The primary contribution of copper in this regard was to improve the diamond retention of the matrix.

Further modifications to the process were made by shifting the debinding step to a separate unit process between the cold press and mROC process. The debinding step was performed in a furnace with a hydrogen atmosphere, and the adhesion between diamond and matrix was improved.

TABLE OF CONTENTS

LIST OF TABLES

LIST OF FIGURES

ACKNOWLEDGMENTS

I would like to express my sincere thanks to my advisor, Prof. Zhigang Zak Fang, for his guidance as the Polaris lighting up my way ahead. His wisdom, professionalism, and work ethic have long been encouraging to me.

My profound gratitude to the members of my thesis committee, Prof. Mark C. Koopman and Prof. Reaz A. Chaudhuri, for their precious advice, time, and contributions.

Genuine gratitude is dedicated to Prof. Ravi Chandran and Prof. Sivaraman Guruswamy, whose kindness and understanding helped me overcome the hard time during and after a horrible car accident of mine.

I would also like to acknowledge the guidance and assistance of Dr. Xu Wang, Yanlu Zhai, and Dr. Chai Ren during the research efforts performed. Additionally, I would like to thank the members of the Fang research group: Kyu Sup Hwang, Jun Guo (Jane), Pei Sun, Chengshang Zhou, Ying Zhang, Jingzhu Li (April), James Paramore, Matthew Dunstan, and Lu Yang. And I also want to thank the members of Metallurgical Engineering Department: Fei Cao, Kay Argyle, Evelyn Wells, and Sara Wilson.

I gratefully acknowledge financial support for this project from Kingdream Public Limited Company.

Genuine thanks to Chai Ren, again, and Quan Shi, for their continuous help, in both academic work and life, throughout my graduate years.

Special thanks to my girlfriend, Yuxiao Lin, for the love, support, and encouragement she has shown throughout my most difficult time.

At last, my deepest gratitude to my parents, Prof. Yuhong Gu and Dr. Jing Li, for their love for each other, for me and for the family.

1. BACKGROUND, SCOPE, AND OBJECTIVE

Hard and ultrahard materials are commonly used in abrasive-wear environments, and many of these have crucial industrial applications, particularly in the areas of rock drilling, mining, and oil and gas exploration and extraction, as well as in metal working and cutting-applications. Such applications require far more than high hardness, however, and generally have a significant list of other crucial properties, including: acceptable fracture toughness, corrosion resistance, and high thermal conductivity, since high heat is generated that must be removed from near the work surface. Composite structures have offered some of the best and most widely used material solutions to these demanding applications over the past 60 to 70 years. In such materials, a very hard abrasion-resistant ceramic, or combination of ceramic phases, is generally combined with a more ductile matrix. Thus, the composite structure takes advantage of the hardness and abrasion-resistant nature of the hard reinforcement, while gaining fracture toughness and resistance to chipping from the more ductile matrix.

One of the most successful examples of such a material has been cemented carbides, where the harder, more brittle phase is tungsten carbide and the ductile matrix is cobalt. Numerous combinations of other carbides, nitrides, and additional ceramic reinforcements within a similar ductile matrix comprise a class of materials known as

cermets.

Composite materials containing diamond, as well as materials with diamond coatings, have been expanding their range of applications over the past 20 years, particularly in high-abrasion wear environments. Diamond-tungsten-metal (DTM) matrix bits for rock-drilling applications, like oil, gas, and mineral extraction, are an example of such a material, and are the subject of the present work. These DTM materials are composed of diamond grit along with tungsten carbide, cobalt, and other metal or ceramic constituents. Key variables desired for high performance include homogeneous distribution of the diamond grit and strong adhesion between the diamond grit and the remaining components, referred to as the matrix.

The central focus of the work presented here involves the independent development of a procedure to produce these samples in the laboratory, since commercial processes are essentially proprietary. In addition to this, limited variations in processing and composition were investigated and analyzed in terms of their effects on diamond adhesion and distribution within the materials produced.

1.1 Oil and Gas Drilling

When an oilfield is discovered via a given geological method (such as seismic imaging, electrical currents, gravitational and magnetic anomalies, etc.), drilling companies will set up several drill rigs for wildcat wells to locate the exact position of the oil reservoir. After that, a drill rig will be built for the production well. As shown in

Fig. 1, the drill bit at the bottom of wellbore, which is mounted on the end of drill strings, is the part of the drill rig that cuts and breaks up the rock formations so that the rock cuttings and sand can be removed.

In rotating drilling, the drill bits are rotated by a turntable rotating the drill string or drill fluid actuating downhole motors, or by both methods. The total weight of drill strings gives the drill bit a downward force to break rocks and create the borehole. The type and quality of drill bits, and characteristics of rocks have a direct influence on the speed of drilling, quality of oil wells, and drilling cost.

The cost of operation for drill rigs (shown in Fig. 1 and Fig. 2 [15]) is striking. Based on the "2015 Well Cost Study" (published by the Petroleum Services Association of Canada, 2015) the daily cost for a drill rig is $18,500 [24].

1.2 Drill Bits

There are four types of bits: roller cone bits, drag bits, PDC bits, and coring bits [25].

A coring bit is used to core sections, cylinders of rock which are removed from the drilling apparatus intact so that they can be analyzed to provide rock characteristics of the formation. Cores are used for analysis, not for wellbore drilling. The shapes of coring bits and wellbore drilling bits are different, but their principles are the same. The present work will focus on roller cone bits, drag bits, and PDC bits, all of which are wellbore drilling bits.

The roller cone bit was invented in the early 1900s by Howard R. Hughes [25], and an example is shown in Fig. 3. The primary thought was to turn the rotation of drill strings into the impingement of bit teeth, and in this way rotating drilling becomes percussion drilling. There are three kinds of roller cone bits: monocone bits, bicone bits and tricone bits. In industry, tricone bits are more widely used than the other two for oil drilling.

Unlike roller cone bits using stress force, the principle of the drag bit, which is shown in Fig. 4, uses shear force to cut rocks [25].

Polycrystalline diamond compact bits (PDC bit) are a generic term for bits using polycrystalline diamond materials as cutting units, and an example is shown in Fig. 5. Subdividing different types of PDC bits via different cutting materials, there are natural diamond bits; PDC bits, which use synthetic diamonds; and Thermally Stable Polycrystalline bits (TSP diamond bits). Only natural diamond bits use naturally formed diamond particles as the cutting material. The operating principle of PDC bits is similar to that of drag bits: both use shear force to break rocks [25].

One disadvantage of PDC bits is that only one side of the insert is involved in the cutting action, rather than the entire diamond compact being subjected to wear operations. This is because the PDC inserts are nearly vertical to the rock surfaces when drilling. Once the diamond compacts are worn on one side, the bit must be removed from the wellbore. Extended life of the bit can then be achieved by simply removing the PDC inserts from the bit and rotating them at an angle so that the unworn side is in the

working direction.

With the demand for fossil fuel increasing worldwide [42], one predominant trend in petroleum drilling is toward deeper wellbores, as nearer surface reservoirs are depleted. Two major problems we need to face are the high down-hole temperature and the high compressive strength of the formation. Deeper wellbores have led to higher down-hole temperatures and higher compressive loads on the drilling bits and, to some extent, harder rock formations being encountered more frequently. Roller cone bits rely on the indentation of rock, and hard formations significantly decrease the rate of penetration. Additionally, the thermal stability of traditional roller cone bits is not as good as TSP bits; PDC shear cutters are too brittle for drilling hard rocks. Because of these, the impregnated diamond bits (impreg bits) have come into the drilling industry's horizon.

The recent invention of an impregnated diamond cutting structure relates mostly to drag bits for oil and gas exploration with diamond-impregnated cutting surfaces in which diamond particles are embedded into the surface. Diamond grit uniformly distributed in a metal matrix can help improve diamond retention and wear life. If the diamond particles are irregularly distributed, there will be diamond clusters and areas void of diamond grit in the matrix. A rich diamond region will show a lack of matrix which leads to the decrease of diamond retention, while the area containing little or no diamonds has poor wear properties [43].

Compared to roller-cone bits and PDC bits, impregnated diamond bits can be applied in extremely hard deep formations, but the rate of penetration (ROP) is very slow.

We can see from Table 1 how the different bits are used.

The DTM insert is used in impreg bits, which is one of its unique features. The insert is made from WC and Co powders mixed with synthetic diamond grit; it has a higher wear resistance than the material of the bits body. Diamond grit protrudes from the matrix alloy and does the major grinding work.

Table 2 shows the conventional superhard materials used in industry; however, these materials are not really optimized; hence, the task required of users here is to find the best combination of the composition that offers the properties needed, both mechanical and commercial.

Impregnated diamond bits, as shown in Fig. 6, are designed for these high-pressure high-temperature working conditions. Compared to PDC bits, another advantage of impreg bits is the extended working life; consequently, impregnated diamond inserts have substantially taken the place of diamond compacts. Impreg bits are composed of millimeter sized diamond grit typically distributed throughout the bulk of a WC-Co matrix, and will be described in more detail below. As the metal matrix (using hard materials, such as WC-Co) and exposed diamond grit are worn away, underlying diamond grit within the matrix will be exposed on the working surface and will continue to facilitate the cutting process. These renewed or regenerated working surfaces containing diamond grit begin another working life cycle. Because the material bulk provides the continuous exposure of new diamond abrasive particles, the life of the bits are extended. Commercially, longer working life of the bits means less down time for

exchanging bits, and thereby saves significant expense for drilling operations [25].

In the early 1980s, TSP came into play, leading to a major change in drill bit technologies for oil and gas drilling. PDC bits have now replaced roller-cone bits in many domains, and now PDC bits account for the majority of the market.

1.3 Hard Materials

Hard materials can be classified as hardmetals, ceramics and superhard materials, which include but are not limited to: carbides, nitrides and borides of tungsten, titanium, molybdenum, chromium, tantalum, niobium and rhenium; as well as cemented carbides; oxides; superhard boron nitrides; diamond; and related compounds [18, 72].

Hardmetals (generally speaking, sintered or cemented carbides or carbonitrides) are produced via powder metallurgy, and cover a range of refractory, hard, or wear-resistant alloys [18]. Carbide particles in hardmetals are bound by binder-phase metal through liquid-phase sintering [18]. The properties of hardmetals may change dramatically with composition [18]. Cemented carbides, WC-Co metal matrix composites, are now widely used for mining tools, cutting tools, and other applications requiring wear resistance. These materials have a set of mechanical properties that are very desirable for a variety of industrial uses including: high hardness, wear resistance, and compressive strength with adequate toughness and transverse rupture strength [26]. The German company “Osram Studiengesellschaft” issued the first patent on WC/Co in 1923 using WC-6 wt% Co while developing a material for the nozzles in the drawing of tungsten wire for light

bulb filaments [6]. Tungsten carbide-cobalt (WC-Co) cemented carbide was invented by K. Schröter in Germany in 1922 [20]. Due to the high hardness, high fracture toughness, high compressive strength, high transverse rupture strength, and thermal conductivity, cemented tungsten carbide is playing an important role in many crucial industrial applications, including wear parts, rock-drilling, and cutting tools.

WC-Co material has a superior combination of properties including:

1) High modulus and hardness
2) High strength (tensile strength is not high)
3) Excellent wear resistance
4) Not as tough as most metals, but tougher than ceramics
5) Good thermal conductivity

Compared to cermets (composites of ceramic and metallic material) and tool steel, the performance of cemented carbides for cutting tools is in between the two [27]. Cemented carbides are generally tougher than cermets, but have lower wear resistance. On the other hand, they are harder and have more wear resistance than tool steel, but do not possess the fracture resistance and thermal conductivity of tool steel [26]. As a primary choice for a ductile matrix in metal-cemented carbides, cobalt can greatly improve the toughness of tungsten carbide. The unique properties of the materials stem from the brittle hard carbides being combed with the more ductile and soft Co binder. The WC-Co materials combine high modulus, high wear resistance, and sufficient fracture toughness. Commercially, cemented tungsten carbides are one of the most

successful and oldest products produced via the powder metallurgy method [26]. Fig. 7 [21] compares the WC-Co properties of its metal alloys and ceramics. The high flexural strength gives the appearance of high toughness (in the strict sense of fracture mechanics) [21]. Fig. 8 [21] illuminates this tendency.

Hardness shows a direct relationship with wear resistance [23]. In industry, people sometimes use hardness to indicate the wear resistance of a material. Due to its high hardness and strength, cemented tungsten carbide shows excellent wear resistance [21]. Thermal conductivity is a crucial property for abrasive wear applications because the heat generated during the wearing process must be moved away from the working surface. Good heat flow of cutting material is required. WC shows higher thermal conductivity than most metals and that of WC-Co is also higher than mixed carbide systems or TiC-Co [22]. But as the Co content in the matrix increases, the thermal conductivity of cemented tungsten carbide decreases [21]. The fracture toughness of WC-Co materials is also controlled by the Co content. Enlarging the mean free path (MFP) through higher Co content can improve the fracture toughness, which can also be achieved to some degree by increasing WC grain, but at the expense of hardness and wear resistance.

Ceramic tools have long been used in human history, dating back to the Stone Age [18]. These inorganic, nonmetallic materials (typically oxides, nitrides, borides, etc) are hard, strong in compression, and resistant to wear and chemical corrosion, but are also brittle and weak in tension [17]. They are produced from minerals or synthetic particles

which will be formed into green samples and then consolidated by high-temperature processing. They can withstand high temperature (1200-1700 °C) [17].

Superhard materials refer to the materials with hardness higher than 40 GPa when measured by the Vickers Hardness Test [16]. They are extremely hard and wear-resistant. Examples include diamond (both natural and synthetic will be discussed in the next section) and cubic (or ultrafine cubic/hexagonal) boron nitrides [18].

Table 3 [19, 21] compares the basic properties of hard materials. Fig. 9 [16] and Fig. 10 [16] show the relationship among hardness, bulk, and shear modulus.

1.4 Diamond-cutting Tools

As an allotrope form of carbon, diamond is the hardest mineral currently known to mankind. It has the highest critical tensile strength for cleavage (perfect octahedral cleavage [40]) and also the highest bulk modulus [28]. It also possesses high thermal conductivity [28] and low coefficients of friction and thermal expansion. Insolubilization of a strong base and acid, such as aqua regia and caustic soda, shows the inertia of diamond to chemical attack by common acids and bases [1]. Due to all these unique features, cutting tools using diamonds as the primary abrasion particles are promising in applications demanding abrasive-wear conditions.

The history of diamond tools goes back to 350 BC, when they were used for engraving [30]. Broken diamond fragments were first employed as a set in iron handles of metal bonded diamond tools [1, 30, 31]. The first description of a primitive diamond

rock drill can be found in Diderot's Encyclopaedia during the 18th century [30]. A century later, in 1862, Leschot of Geneva developed a complete drilling rig which brought practical application onto a broader scale [30, 31, 32]. In 1883, the concept of bonding diamonds with fine powders was introduced [33]. Both phenolic resin and metal powders, such as brass and iron, were used [33]. This means of consolidation was limited to cold pressing at that time [41]. It was not until the 1930s that hot pressing was incorporated into the impregnation of diamond cutting tools for industrial applications [30]. The development of diamond tools, however, remained limited due to the production rate and price of mined natural diamonds. After the synthetic diamond was invented and developed, the use of diamond tool manufacturing technology accelerated. Now, the synthetic diamond supply represents more than 95% of all industrial diamond consumption [34].

Diamond cutting tools can be fabricated by means of powder metallurgy. The practice of bonding diamond grits using metal powders dates back to 1883 [33]. Classification of diamond tools can be based on the quantity of diamonds involved in the tool, application of the tool, internal structure of the tool, tool type, etc. [1]. Based on tool types, the categories of diamond tools can be listed as loose diamond abrasives, single crystal diamond, bonded diamond grits, polycrystalline diamond (PCD), and chemical vapor deposition (CVD) diamond [1].

Loose diamond abrasives or loose diamond micron powder (natural and synthetic) are the simplest diamond tools [1]. Liquid diamond suspension for polishing is one

example of this kind of diamond tool. Although various sizing criteria and techniques are used, the micron powder is normally defined as a powder finer than 84 μm [50]. Important applications for this kind of diamond tool are polishing gemstones, metal alloys, and ceramic specimens; the finishing of diamond cutting tools; hardened steel, and WC tools [51, 52, 53].

The development of single-crystal diamond tools was restricted before the synthetic diamond was invented because of the irregular size and quality of natural diamonds. Currently, applications of both natural and synthetic single-crystal diamond tools are for use as cutting blanks, wire-drawing dies, and dresser logs [1].

Bonded diamond grits and powders are composites for the largest group of diamond tools used in workpiece-machining applications so far [1]. Both monocrystalline and polycrystalline diamond particles can be utilized. These particles are embedded in a metal or nonmetal matrix. They are embedded into electroplated tools, vitrified bond tools (grinding single-crystal and PCD diamond tools [60], cemented carbides and ceramics [61]), resin-bonded tools (grinding cemented carbides [62, 63], oxide and nonoxide ceramics [64, 65], glass [65], and are used in the fine-grinding and polishing of stones [66]) and for use in metal-bonded tools (tools with a diamond-impregnated working layer) [1].

PCD is produced by consolidation of high-quality and accurately sized diamond powder together with metallic or nonmetallic binder phase at 1200-1600 °C and 6 GPa pressure [54]. Finer PCD grains lead to higher toughness and better surface finishing,

while coarser grains result in higher wear resistance [1]. Cobalt is added as a binder phase for its ability to promote the conversion of graphite into diamond through a dissolution-reprecipitation process [1]. Silicon is sometimes utilized instead of cobalt to achieve better thermal stability [55, 56]. Applications for PCD are demanding, such as the high-temperature drawing of wire (utilizing wire-drawing dies) [67]; the machining of metal matrix composites, fibre-reinforced plastics, high SiAl alloys and abrasive wood composites (carbide-backed blanks) [68, 69, 70]; as well as rock drilling (TSP bits) [71].

CVD diamond is the deposition of metastable polycrystalline diamond film from a gaseous phase onto a suitable substrate maintained at between 700–1000 °C [57, 58, 59]. During the deposition process, no metal catalysts are utilized, so no metallic inclusions are in the CVD diamond, and the CVD diamond is thermally stable [1]. CVD diamond film is used to coat free-standing plates and other coated tools (drills and turning inserts) [1].

The processes for manufacturing diamond tools include but are not limited to matrix powder preparation, diamond and matrix mixture preparation, cold-press, sintering, hot-press, and hot isostatic pressing. People sometimes use the infiltration process to make rotary surface-set diamond bits, TSP bits, and TSP hybrid bits [1].

The matrix powder preparation process with granulation step is used for protecting the composition from the nonuniform random distribution of matrix powders. The diamond and matrix mixture preparation process has the same purpose, but this process aims at the uniform distribution of diamond particles into the matrix [35, 36, 37, 38].

The cold-press/sintering process and the hot-press process both aim to achieve near-full dense consolidated products [1]. Matrix hardness decreases when promoting recrystallization and grain growth takes place during the sintering process in a hydrogen atmosphere. Distortion also happens during sintering [39].

Hot-pressing using a steel die can avoid sample distortion, but nonuniform temperature distribution across the die is a common problem, which can lead to regions with less strength in final products. The process is modified by using die pressing in a furnace; it also combines a debinding step simultaneously.

1.5 Research Objectives

1.5.1 Problems and Challenges

In deep oil wells, high down-hole temperature and high compressive strength of the formation are two common problems. Roller cone bits have good toughness and impact strength but don't have excellent wear resistance; PDC bits have adequate wear resistance but the toughness and impact strength are not very good. So we use impreg bits for drilling deep wells.

In the matrix of impreg diamond inserts used in impreg bits, fracture toughness is inversely proportional to wear resistance, which is the primary characteristic sought for rock drilling. So, increasing fracture toughness to avoid fracture failure will consequently lead to a decrease in both wear resistance and hardness. A trade-off must be made that meets the specific environment of rock drilling applications.

Another major problem is the distribution of diamond grit in the metal matrix. Several methods of making inserts with uniform structure have been attempted. One of these methods uses sonic waves to shake a wet mixture of diamond grit and matrix powders, encouraging the formation of a homogeneous wet mixture (DTM mud). Unfortunately, the diamond distribution can be disturbed when the mud is transferred into other containers during processing.

Therefore, efforts have shifted toward producing dry DTM units, which are pellets that contain a single diamond grit coated with matrix powder. The ratio between diamond and matrix is, in this case, exactly the same as the final products. This method is termed a “pellet-making” approach. A necessary goal of developing a viable process for producing the pellets involves evenly distributing the matrix around each diamond grit, as well as producing pellets of nearly the same size. The approach we used involves the use of a rubber vibrating bowl combined with the use of an appropriate binder at functional volume percentages.

Temperature and pressure are the two key parameters for the modified rapid-heating omnidirectional compaction (mROC) process. Adequate pressure can readily be provided, but temperature introduces several issues. Since the consumables used during the mROC process are single-use, the current is difficult to control when flowing through consumables such as graphite set, steel rings, and titanium discs. An internal resistance difference of different steel rings or titanium discs exists, but the influence can generally be treated as negligible. For the graphite set, which will crack when the upper punch

contacts the pyrophyllite assembly, the operator must set the loads used to close the circuit and seal the internal system. Differences in resistance can be significant between operational runs. The direction and number of cracks within the graphite set cannot be controlled, and internal resistance will increase rapidly if graphite fragments are not in good contact, especially when insulating glass powders enter into the cracks. The influence on current will affect heating temperature as well as the degree of sample sintering. This is the greatest challenge to mROC processing, which aims to produce full density in these materials.

Several trials of temperature tests were run, but none of these could successfully provide a temperature value which gave high confidence. Therefore, the temperature could only be estimated based on experience.

1.5.2 Scope

In the future, the ultimate goal of this application of DTM inserts, which are cylindrical cutters, will be to produce inserts that can maximize the rate of penetration (ROP), which is sometimes a limiting factor for these bits. To eventually reach this end, the designed DTM materials should have the crucial properties of:

1) Homogeneous diamond distribution in the matrix
2) Strong diamond adhesion to matrix
3) High matrix hardness

Within impregnated diamond inserts, diamond grit is embedded in a metal matrix, a

schematic illustration of which is given in Fig. 11. The matrix should have good bending and impact strength, as well as adequate interface strength to hold the diamond particles, but it should also be somewhat compatible in wear properties in order for wear to occur at a vaguely similar rate as that of the area with diamond loss.

It is well known that diamond has the highest hardness among all of the bulk materials in nature. Given that the matrix material should have high hardness and wear resistance, Diamond-Tungsten-Metal Matrix (DTM) composite is a common choice.

In these materials, the diamond particles at the surface are worn away or pulled out, but then new diamond particles in the bulk of the material are exposed to the working surface and, thus, continue to provide ultra-hard wear resistant properties.

1.5.3 Objectives

In this research, we want to develop a manufacturing process to produce DTM inserts which can solve the problem of irregular diamond distribution in a matrix and test the properties of produced sample inserts.

We also want to study the influences of both diamond volume percentage and matrix composition on mechanical properties, specifically matrix hardness.

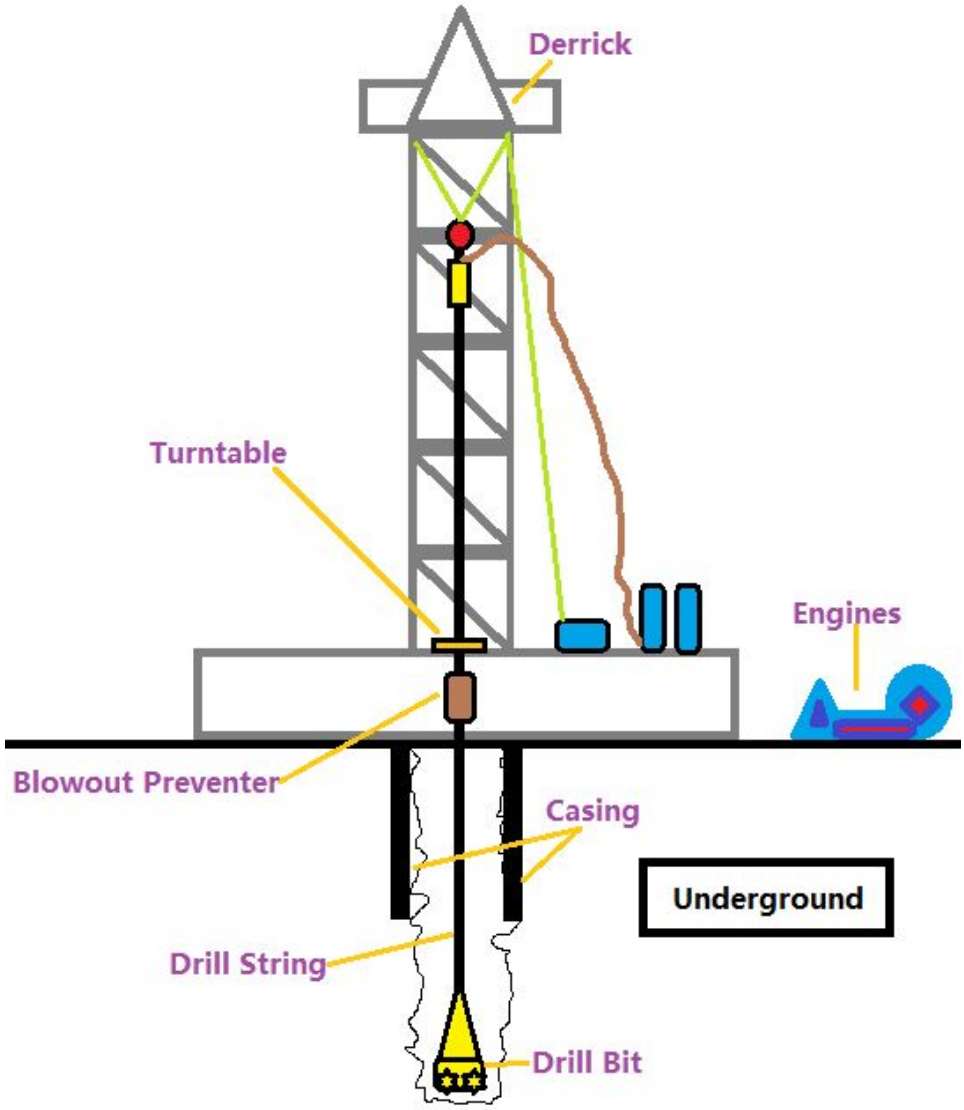

Fig. 1: Schematic diagram for onshore drill rig.

Fig. 2: Photo of onshore drill rig [15].

Fig. 3: Photo of tricone bit.

Fig. 4: Photo of drag bit.

Fig. 5: Photo of PDC bit.

Fig. 6: Photo of impregnated diamond bit.

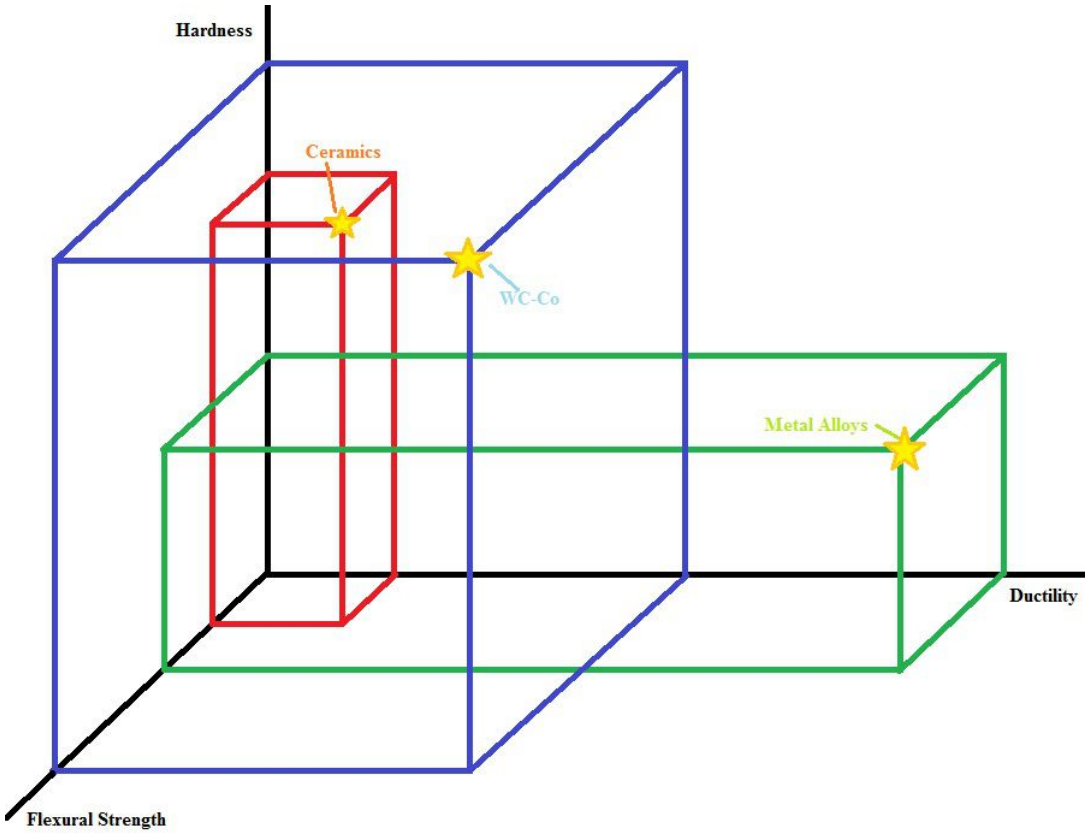

Fig. 7: The relationship between hardness, ductility, and flexural strength; comparing WC-Co, metal alloys and ceramics. Adapted from [21].

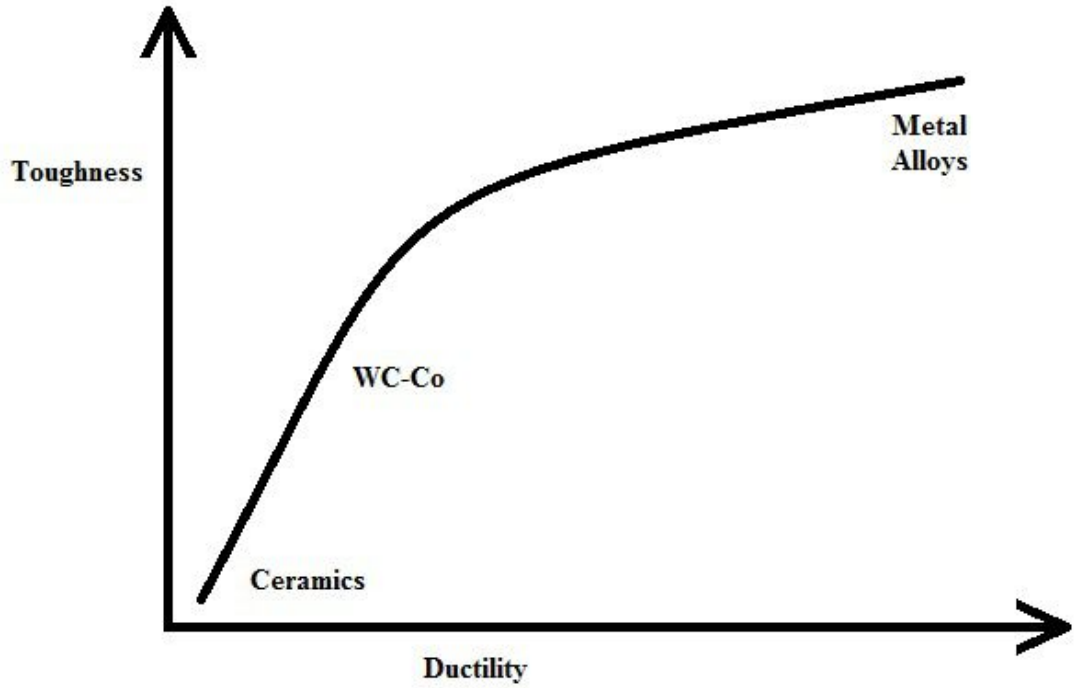

Fig. 8: Comparison of toughness of WC-Co, metal alloys and ceramics. Adapted from [21].

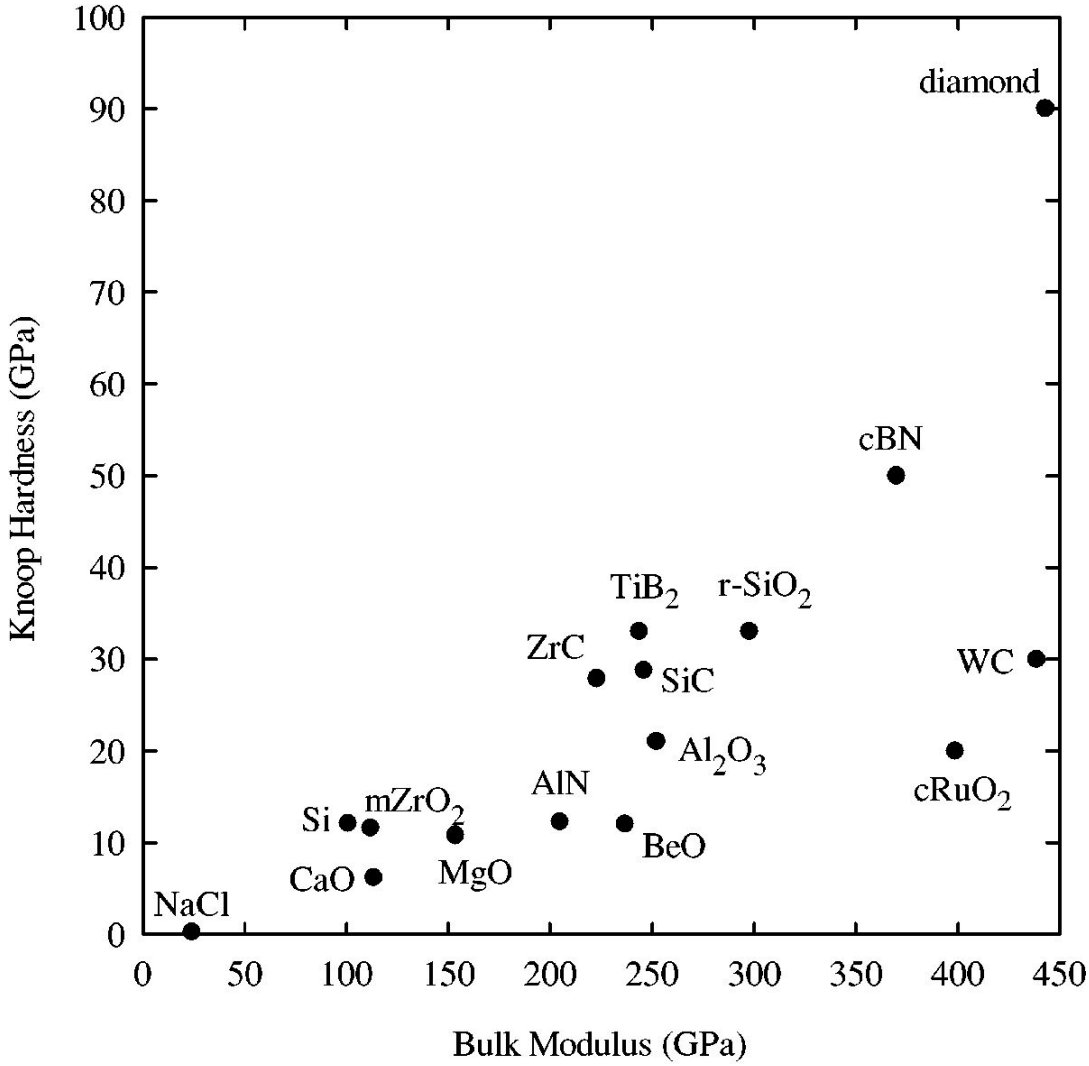

Fig. 9: Relationship between hardness and bulk modulus (r-, rutile-type; c, cubic; m, monoclinic) [16].

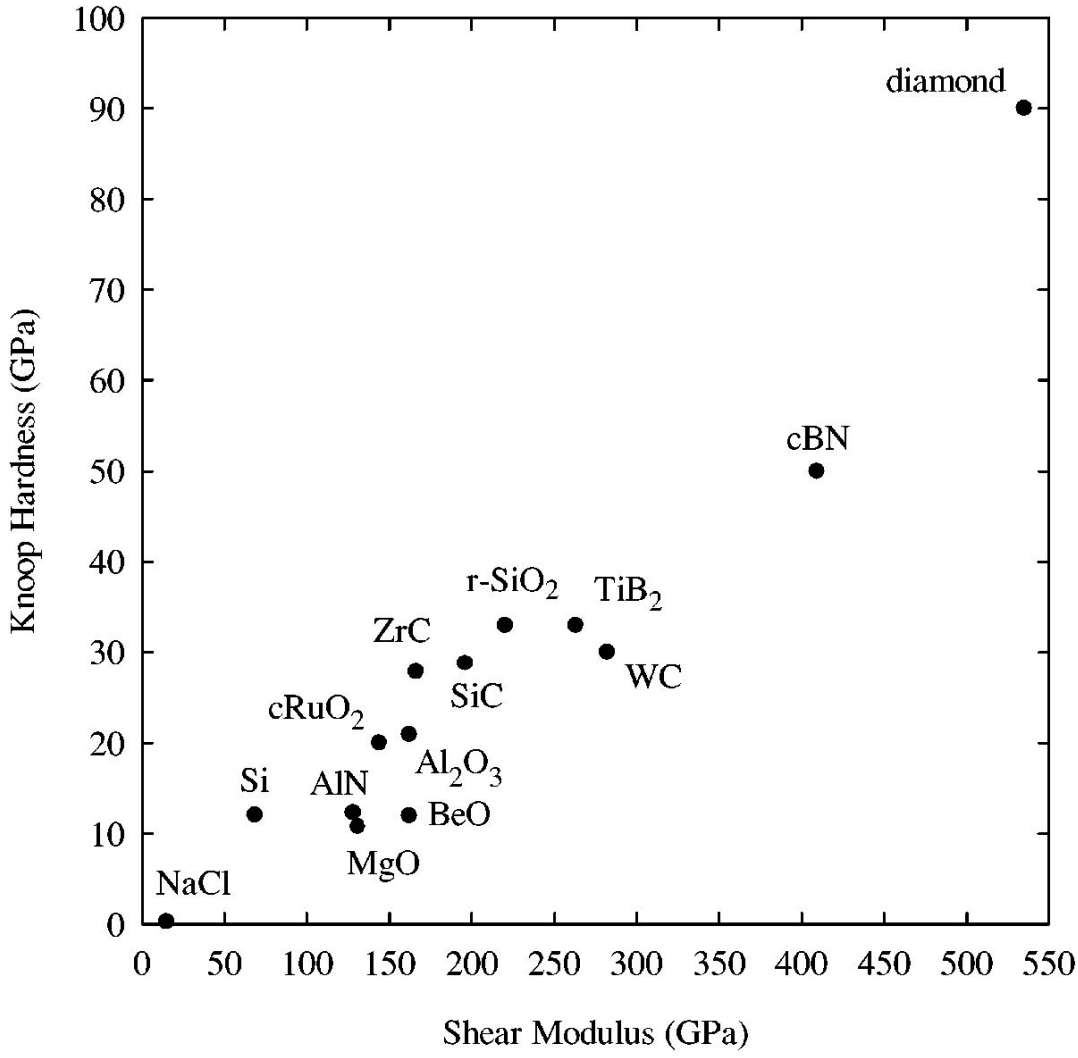

Fig. 10: Relationship between hardness and shear modulus (r-, rutile-type; c, cubic) [16].

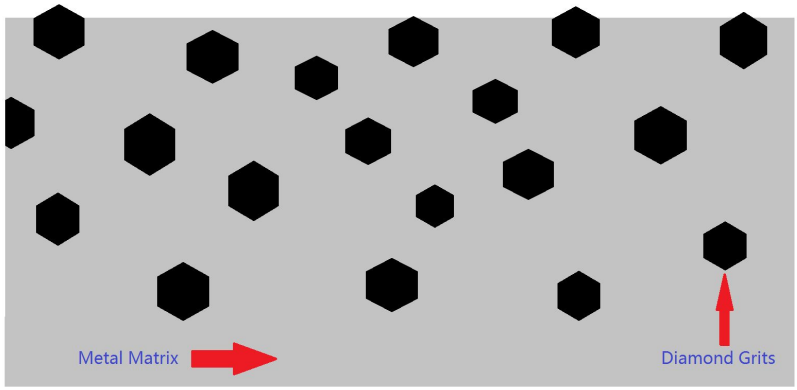

Fig. 11: Schematic diagram shows cross-section of the designed DTM insert.

Table 1: Working parameters of different types of drill bits

	Roller Cone Bits	**PDC Bits**	**Impreg Bits**
Typical Applications	Soft to hard formations	Soft to medium formations	Extremely hard deep formations
ROP	Good - Excellent	Good - Excellent	Very slow
Durability	Moderate	Excellent	Excellent
Impact Resistance	Good	Moderate	Moderate

Table 2: Mechanical properties of conventional superhard materials

	PDC (Polycrystalline Diamond)	**Impregnated diamond**	**DTM**	**WC-Co (Cemented tungsten carbide)**
Flexural Strength	Medium (200 ksi)	Low (100 ksi)	Medium	High (400-500 ksi)
Fracture Toughness	Medium (~10 MPa√m)	Low	Medium (~10 Mpa√m)	High (10-20 MPa√m)
Wear Resistance	High	Low	Medium	Medium
Abrasive Cutting Capability	Unknown	High	High	Low
High Temperature Strength	High (but thermal stability is an issue)	Very Low	Low	Medium

Table 3: Basic properties of hard materials [19, 21]

	Vickers Hardness, Hv	Young's Modulus, GPa	Compressive Strength, MPa
High-speed steel	750-800	210	3500-4000
WC	2200-3600	625-700	3350-6830
Cemented carbides, WC-Co	700-2200	400-680	3000-9000
TiC-based cermets	1500-2200	300-450	3000-5000
SiC	2300-2600	400-460	1000-4500
Ceramics (oxides, nitrides)	1500-2500	300-400	3000-4000
Al_2O_3	1200-2060	343-390	500-2700
Polycrystalline cubic boron nitrides	4000	680	6000
Polycrystalline diamond (PCD)	8000	850	7600

2. PROCESS DEVELOPMENT

2.1 Material Preparation

This section includes details of the materials and processes used in the current study. As mentioned earlier, the development of this procedure was the core of the project.

Diamond grit was provided by Element 6 Composites (Elbridge, NY, USA), and ranged in size from 400–600 μm in diameter. The diamond grit was coated with TiC by the manufacturer. Sorting of the diamond particles by size was performed using a two-step procedure: 1) by manually shaking the particles and then 2) by using a dual-drive vibratory laboratory ultrasonic shaker (HK Technologies Inc., Warwickshire, UK). In this step, the diamond grit was sieved with 30, 35 and 40 U.S. mesh sieves for both sorting methods and divided into four groups:

1) Particle size below 400 μm
2) Particle size between 400 to 500 μm
3) Particle size between 500 to 600 μm
4) Particle size above 600 μm

Only the two groups with particle sizes between 400 and 500 μm and between 500 and 600 μm were used for these experiments. The two groups of diamond were marked as BD (size range from 500 to 600 μm) and SD (size range from 400 to 500 μm).

Tungsten carbide powder for this study was made by Buffalo Tungsten Inc. (Depew, NY, USA) with an average particle size of 0.36 μm; cobalt powder was from the same company with an average particle size of 1.53 μm. Copper powder with an average particle size of 44 μm was purchased from Chemical Store Inc., which is known as ChemicalStore.COM (Clifton, NJ, USA). The mixed raw materials were milled with a Szegvari Attritor Grinding and Dispersing Mill (Union Process, Inc., Akron, Ohio, USA). In this step, 222 g of powder mixture and 6.5 mm tungsten carbide satellites were loaded in a stainless steel milling canister with a ball-to-powder ratio of 3:1, along with 140 mL of ethanol. The milling time used for this work was five hours and the milled powders were then dried in a BÜCHI Rotavapor R-200 (BÜCHI Corporation, New Castle, DE, USA). The dry mixture can be directly used in the pellet-making step.

The binder liquid was prepared by dissolving saturated-level Polyvinyl Alcohol (PVA, in powder, from The Chemistry Store.COM) and 5.556 x 10^{-5} mol/L Polyvinylpyorrolidone (PVP, in powder, from Fluka via Sigma Aldrich, St. Louis, MO) into ethanol with assistance of rotor and heating pan. This binder is used for bonding dry powders onto diamond grit.

2.2 Pellet-making Process

In our process development, the preparation steps for matrix powder and diamond/matrix mixtures were combined as one granulation process of which the matrix powder of the DTM composite was coated diamond grit. Thus, each individual pellet

contained a composition exactly the same as the final product. As green samples were made by means of cold-press using pellets obtained from a previous step, the consolidation process followed.

The flowchart of the pellet-making process is shown in Fig. 12. WC and Co powders were mixed and milled, utilizing ball milling. Then, the powder mixture was coated onto diamond grit with the assistance of binder liquid in a vibratory tumbler. Finally, pellets with adequate size were obtained after the coating/granulation step. The Bel Air Vibratory Tumbler (Bel Air Finishing Supply, Corp., North Kingstown, RI, USA) with rubber shaking bowl on top used in this process is shown in Fig. 13. The detailed procedures are discussed in the following sections.

2.2.1 Addition of Binder Liquid

Diamond grit (20 g per trial of pellet-making process) was shaken in the rubber shaking bowl (red part) with the binder liquid sprayed onto the diamonds manually. Each cycle took three iterations of spraying. The spraying was followed by a 30 second gap and this step was repeated in 2 to 3 cycles.

2.2.2 Addition of Matrix Powders Mixture

After adding binder liquid, the circulation step was performed following the procedures described below:

1) Binder liquid was sprayed once.

2) About 2 g dry powder mixture was spread over the diamond grits. A spatula was

used to spread the dry powder mixture; then, another 2 g of powder was spread when no obvious powder could be seen shaking in the rubber bowl. The spreading action and addition of powder was repeated 2 to 3 times.

3) Steps 1 and 2 were repeated three times; then, the vibratory machine was turned off, and pellets were air-dried.

4) The dried pellets were manually divided into six groups based on size (details shown in Table 4) by sieving using U.S. mesh sieve sizes of 40, 35, 30, 25, 21, 19, 18 and 16. The small pellets without diamond grit core (size < 0.4 mm) and large pellets formed by multiple small granules (size > 1.18 mm) were washed with an ultrasonic cleaner and the diamond grits were recycled. Tiny powder granules were formed that were smaller than 0.4 mm. These were too tiny to be used for further experiments. Pellets larger than 1.18 mm were checked to discern whether they were caused by multiple small granules joined together. These big particles were either broken into small individual ones or an ultrasonic cleaner was applied to wash powders on the pellets away, whereby fine diamond grit was obtained.

5) The percentage of pellets with diamond cores was analyzed by randomly examining 100 pellets. The batches with a percentage above 93% were selected for the following steps while the others were recycled and washed by means of ultrasonic cleaner for obtaining fine diamond grit.

6) Pellets with sizes ranging from 0.9-1.0 mm in diameter (Group 6) were marked as SP while those with sizes ranging from 1.0 to 1.18 mm (Group 7) were marked as BP.

The qualified pellets (SP and BP) were collected, and the rest were pulled back into the rubber shaking bowl by sizes, and Steps 1 to 5 were repeated.

The morphology of diamond grit and pellets are shown in Fig. 14.

2.3 Green Samples

Twenty grams of pellets were cold uniaxial-compacted using a cylinder-shape steel die with a pressure of 200 MPa and holding time of 5 min. The standard green part dimension was 20 mm in length. An average height shrinking ratio of 75% could be expected during the mROC process, with small variations between different sample compositions (a disparity of less than 1 mm was observed). The estimated final sample length was 15 mm.

2.4 Modified Rapid Omnidirectional Compaction (mROC) Process

The modified rapid omnidirectional compaction (mROC) process was used for consolidation of the composite materials. The mROC process was provided with most of the advantages of hot-press and the hot isostatic pressing (HIP) process. Improvement was made by adding the debinding step to HIP instead of presintering in a furnace and highly increasing the pressure to around 560 MPa. Duration for the operation was reduced to five minutes to avoid diamond graphitization.

The mROC process is a quasi-isostatic consolidation process used to densify powders by using rapid heating (temperature increases over 100 °C/min) and ultrahigh pressure (above 400 MPa). The maximum working temperature ranges from

1000–1100 °C, the maximum pressure is 560 MPa, which is comparable to the commercial Hot Isostatic Press (HIP) processes.

The high-pressure punch and steel pedestal are applied to the top and bottom of the pressing die with electric power supply cables connected to both ends as a heating system. As shown in Fig. 15, during the mROC process, electric current flows through the pressing system, which includes an upper punch, steel ring, titanium disk, graphite cell, and lower punch. The sample temperature is increased by resistance heating. The maximum powder supply of an mROC system is about 6 KVA. The glass inside the sample package is melted by the resistant heating, which provides a quasi-isostatic pressing condition. The thermal and electrical insulating pyrophyllite sleeve and pucks are pressure sealed.

The mROC process consists of three steps, as shown in Fig. 16: preheating, pressing, and cooling. In order to realize the quasi-isostatic pressure effect, glass inside the graphite cell is molten first by applying 85% output of the total power capability for five minutes. The molten glass functions as the pressure transmit media. Finally, the compression step is applied. After the pressure is slowly increased to 90 short tons, current must be controlled inside to a range of 650 to 720 A by adjusting output power.

2.4.1 Green Sample Preparation

1) The steel high-pressure punch, puck, and pedestal were polished using abrasive sand paper.

2) The green part was covered with graphite tape to avoid exposure to open air.

3) The Boron Nitride Aerosol Lubricoat provided by ZYP Coating Inc. (Oak Ridge, TN, USA) was sprayed uniformly as a lubricant onto the surface of both the pyrophyllite sleeve and the covered samples.

4) Two coated samples were placed into one graphite cup.

5) Samples were placed at the center of the cup without contacting each other or the internal wall. The surrounding space was filled up with compacted glass powders densely. This can be done by slightly pressing the samples and glass powders.

6) The graphite cup was sealed with a graphite lid. Then the set was slid into the pyrophyllite sleeve with the lid facing up.

7) Pyrophyllite pucks were embedded into steel rings, and split annular mica slices were clipped by two titanium disks.

8) All of the above units were assembled together and placed onto the small steel puck on the steel pedestal, then covered by the steel die.

2.4.2 Assembly

The whole assembly was loaded into the uniaxial press and sealed by lowering the upper punch. The system was then purged by repeating vacuum and flowing argon (Ar) three times. Then, a vacuum machine was turned on and operated throughout the whole mROC process. Ar gas was selected for purging after vacuuming for 30 minutes. This step was repeated twice before Ar flow was shut down.

2.4.3 mROC Process

The system was cooled by flowing water during the operation.

The heating machine was turned on with an output set to “45” (based on a total range from 0 to 105). This represents the output percentage. The load was increased continually from 0 short tons until the current presented. The maximum load limit in this step was 20 short tons.

The green part was first debinded by keeping the system at “60” for 30 min.

In the next step, by raising the output to “85” for 5 min, all glass powders were made molten and a quasi-isostatic pressure environment in the graphite cup was achieved.

After the glass was fully molten, the pressure was slowly and continuously increased to 90 short tons. An increase of current can be observed as a result of pressure rising, which caused a decrease of resistance in the system. During the high-temperature and high-pressure compaction, system output was adjusted carefully to keep the current inside the range at 650 to 720 A. A small variation may be observed as a result of uncontrollable random resistance.

After five minutes of high-temperature, high-pressure compaction, the heating machine was shut down and the whole system was cooled with pressure still being applied.

The load was removed after 15 minutes of cooling. Then the DTM insert was obtained.

2.5 Sample Preparation

2.5.1 Mounting

The sample was mounted inside the compression mounting compound using a Buehler Simplimet 1000 automatic mounting press (Lake Bluff, IL, USA).

2.5.2 Surface Grinding

Seen from both ends of the cylinder insert, surfaces are not flat and diamond grit with a thin layer of matrix are extruded. During the mROC process, coated matrix powder was pressed towards the core of the cylinder and the outer diamond particles were exposed. This action resulted in a no-matrix layer with exposed diamonds on the surface followed by a matrix-rich layer underneath.

In order to reach a “diamond-metal matrix uniformity” layer and get reliable results, a 1 to 2 mm grinding depth was necessary for both sides.

A rough surface grinding was performed on the top and bottom sample surfaces using a Norton 150-grit diamond surface grinding wheel and Chevalier high-precision surface grinder.

2.5.3 Polishing

In order to improve the metallographic and hardness test results, the sample was polished using a MetPrep 3 grinder/polisher with PH-3 power head (Allied High Tech Products Inc., Rancho Dominguez, CA, USA) to remove surface scratches.

The rough-polishing step had 3 stages and used water as the polishing solution.

Apex diamond grinding discs (DGDs) of 240, 125, and 9 μm provided by Buehler were used in descending order, according to size, as listed in this sentence. Rolling speed was set to 400 rpm, and 30 minutes of polishing was required when using each grinding disc.

A subsequent fine polishing step was required right after the rough polishing. Instead of DGDs, polishing papers were used. The scale grades of MetaDi monocrystalline diamond suspension were 9, 6, 3, 1 μm made by Buehler, and the required polishing time was 40, 30, 30, and 30 minutes, respectively.

2.6 Evaluation Test

The evaluation tests for physical and mechanical properties included a density test, diamond distribution test, Vickers hardness test, and microstructure images capture. The images of the polished surfaces were taken by optical microscopy and the diamond volume percentage was calculated based on the image viewed according to a point-by-point method. Sample density was measured by the Archimedes method. Sample hardness was analyzed by Vickers' hardness method using The Leco Vickers Hardness Tester LV700AT, and the metallographic observations were performed using FEI NovaNanoSEM scanning electron microscope (FEI, Hillsboro, OR, USA).

2.6.1 Density

Volumetric mass density is calculated based on mass per unit volume as shown in the equation below [11].

$$\rho_{\text{sample}} = \frac{m_{sample}}{V_{sample}}$$

where

ρ_{sample} is the density of sample

m_{sample} is the mass of sample

V_{sample} is the volume of sample

The Archimedes method was used to characterize the sample density. After fully immersing the sample in the liquid, the buoyant force on the sample is equal to the gravity force of the displaced water [11]. Thus, in our case, the volume of the immersed sample is equal to the volume of displaced water. The negative values gained from the balance scale is the weight of displaced water. Then the volume can be calculated by simply using water weight dividing by water density.

$$\rho_{\text{sample}} = \frac{m_{sample}}{V_{sample}} = \frac{m_{sample}}{\left| m_{apparent,negative} \right| / \rho_{water}}$$

where

ρ_{sample} is the density of sample

m_{sample} is the mass of sample

V_{sample} is the volume of sample

$M_{apprent,\ negative}$ is the value obtained from balance scale

ρ_{water} is the density of water

2.6.2 Diamond Distribution

The point-by-point method is based on the assumption shown in the equation below. The ratio of the point number in the object region (as it relates to the total point number on the surface) is equal to the ratio between the area of the object region and the total area [14].

$$P_P(\frac{mm^0}{mm^0}) = L_L(\frac{mm}{mm}) = A_A(\frac{mm^2}{mm^2}) = V_V(\frac{mm^3}{mm^3})$$

where

P_P is the ratio of number of points in a certain area to the total number of points

L_L is the ratio of a length of line in a certain area to the total length of the line

A_A is the ratio of object area to total area

V_V is the ratio of the object volume to total volume

When counting points, the points in the object region count as 1.0 and the point on the edge counts as 0.5. The resulting accuracy has been further improved by replacing the 0.5 with an estimated proportion value for the edge points.

2.6.3 Hardness

The Vickers hardness test was performed using the Leco Vickers Hardness Tester LV700AT. Extremely accurate hardness readings can be gained from the Vickers hardness test because it gives nearly equal readings when testing the same point on a uniform material with a variety of loading settings for each test trial [12].

The method indents the test material with a diamond indenter. The indenter is a

right pyramid diamond with a square base and an angle of 136° between opposite faces, as shown in Fig. 17. Range of applying load is between 1 to 100 kilogram-force. We were using a load of 2 kg, which was applied for five seconds. After the load was removed, the two diagonal lengths of the indentation were measured using the scanning electron microscope, and the sloping surface area of indentation was calculated based on the average diagonal length. The Vickers Hardness Value is the ratio of load applied (in kgf) and the area of indentation (in mm^2) as described in the following equation [12]:

$$H_V = \frac{2F * \sin\frac{136°}{2}}{d_{average}^2} \approx 1.854\frac{F}{d_{average}^2}$$

where

H_V is the Vickers Hardness

F is the loaded force

$d_{average}$ is the average length of the two diagonals

The random distribution of diamond grits inside a WC-Co matrix may introduce significant error into results, as the hardness will dramatically increase in the areas near or above diamond grits. To minimize this effect, the Vickers Hardness Test was only performed in the areas between the diamond grits and a relatively low load of 2 kgf was used.

2.6.4 Test of Microstructure

The microstructures of the matrices were studied using the FEI NovaNano Scanning Electron Microscopy (SEM). Pictures of the fracture surfaces were taken with magnifications of 70x, 100x, 300x, 1000x, 1300x, 5000x, 8000x, 10000x, 16000x, 30000x, and 80000x.

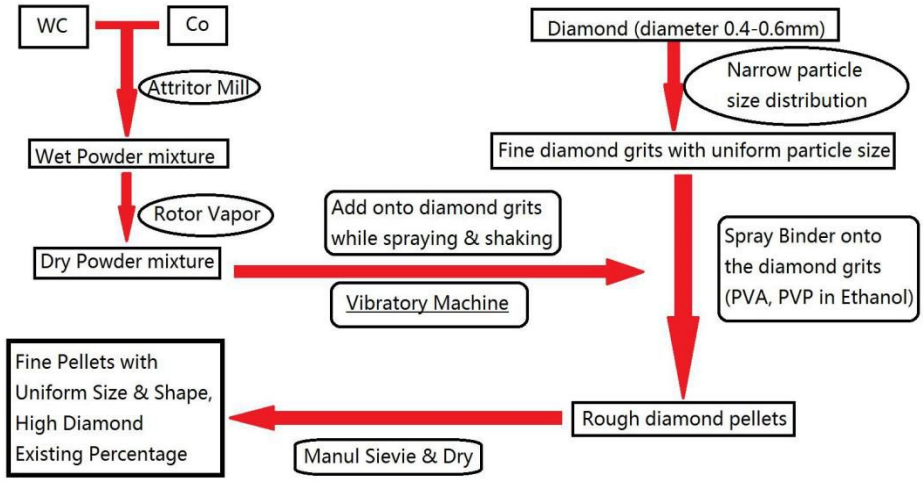

Fig. 12: Flowchart briefly shows the pellet-making process.

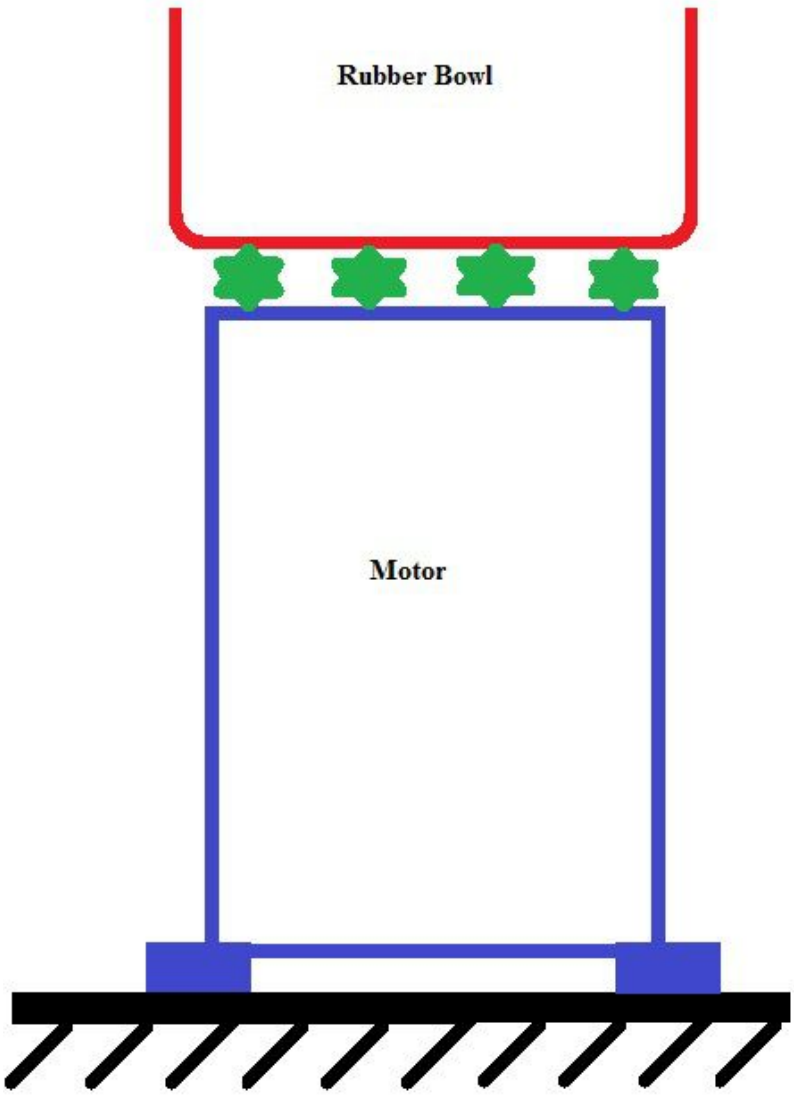

Fig. 13: Bel Air Vibratory Tumbler with rubber shaking bowl on top.

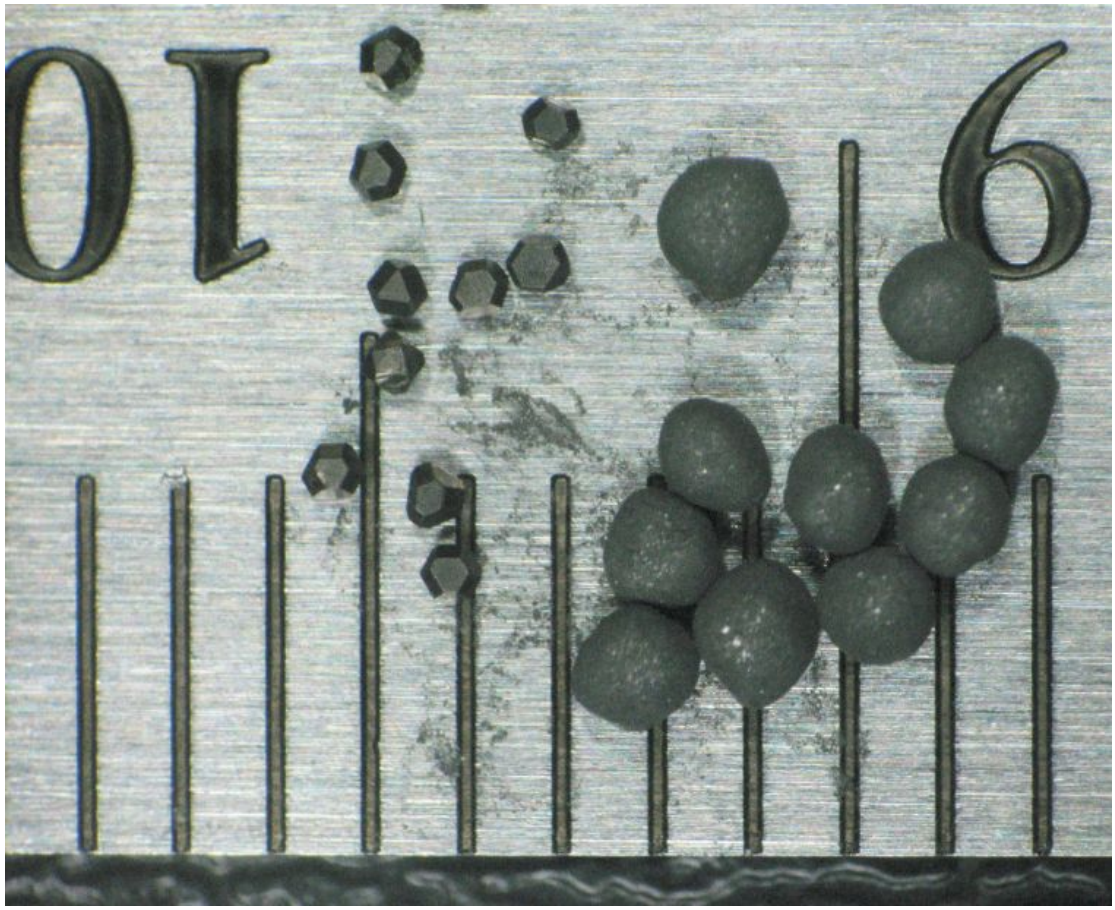

Fig. 14: Picture showing the morphology of diamond grit (left) and pellets (right).

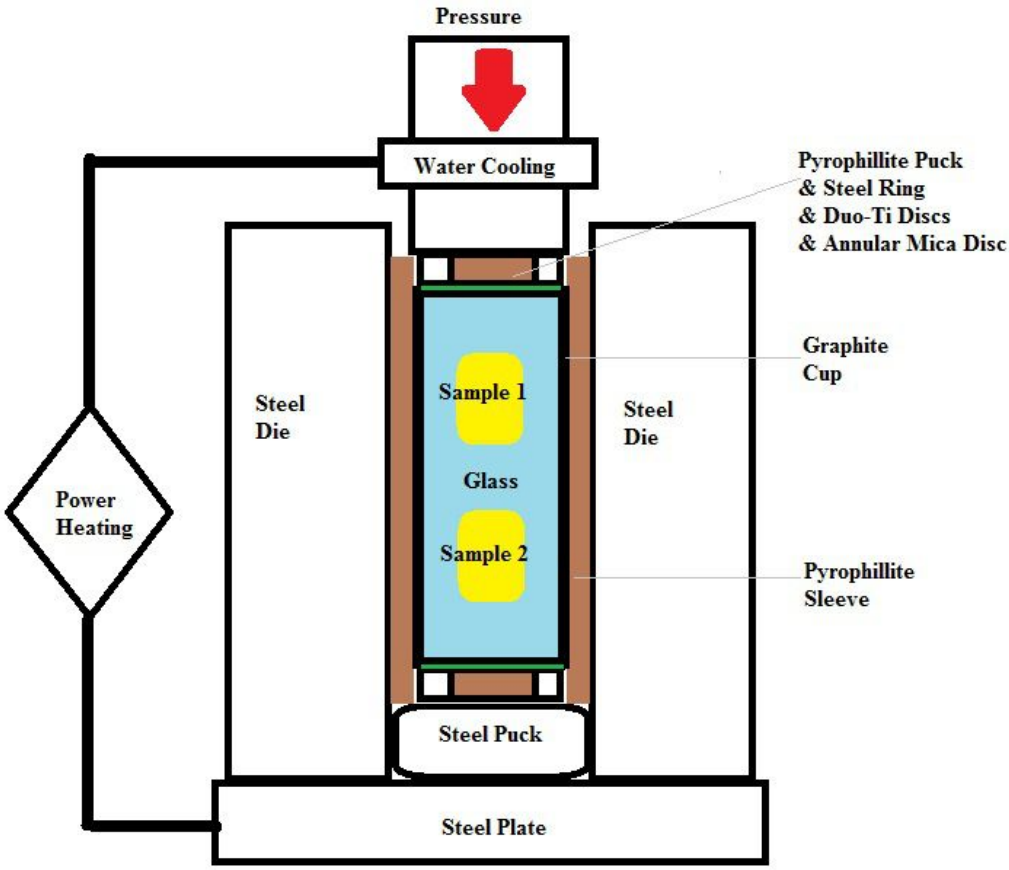

Fig. 15: Cross section of overall hot-press equipment.

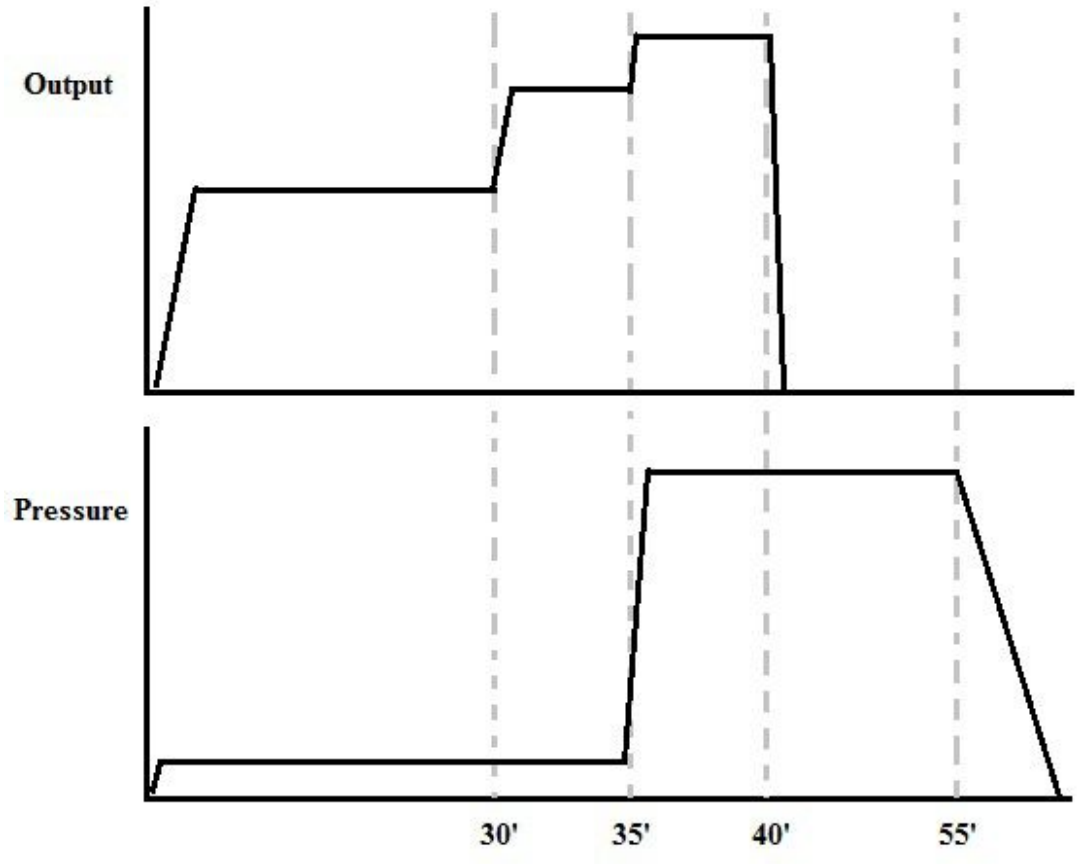

Fig. 16: Plot describes modified rapid-heating omnidirectional compaction (mROC) process.

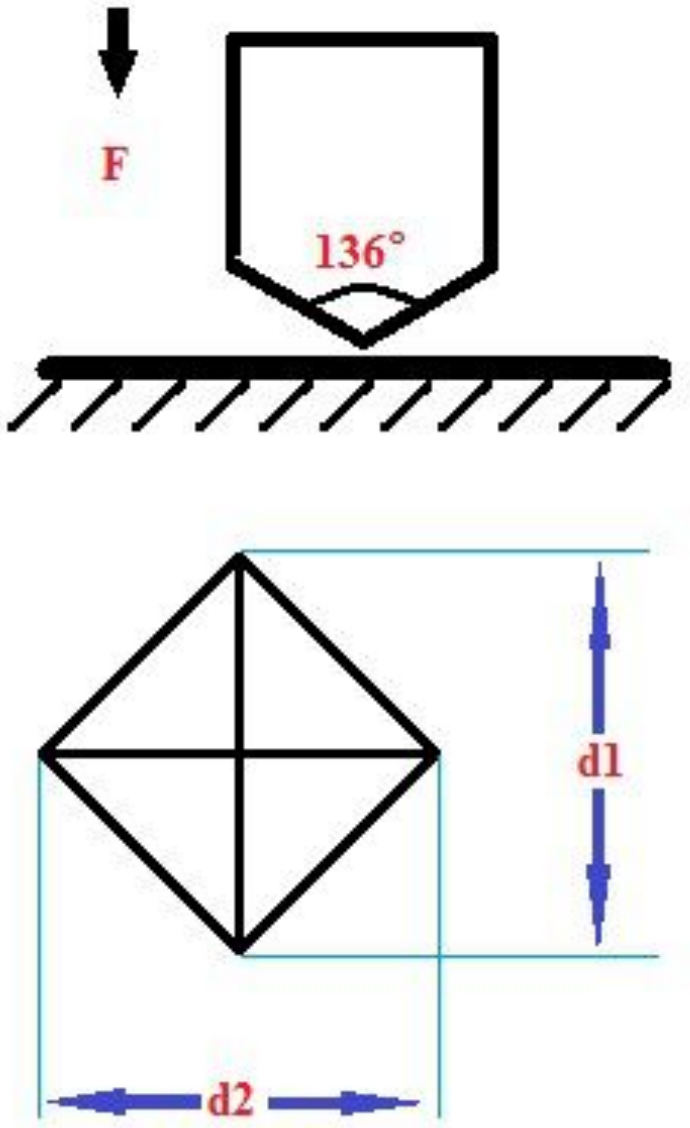

Fig. 17: Schematic diagram for Vickers Hardness Test.

Table 4: Six groups of pellets determined by size after manually dividing

Group No.	Size range, mm
1	0.4-0.5
2	0.5-0.6
3	0.6-0.7
4	0.7-0.8
5	0.9-1.0
6	1.0-1.18

3. DESIGN OF DTM COMPOSITE, FABRICATION OF SAMPLE CUTTERS, MICROSTRUCTURES, AND PROPERTIES

3.1 DTM Composite Design

The metal matrix of the diamond-tungsten-metal (DTM) insert is the key to impreg bits' quality. This matrix is used to enclose the diamond particles. A working environment with erosive action was produced by rock formation, rock cuttings, and drilling fluid. In this working condition, drill bits also need to undergo high temperature and high pressure caused by abrasion and the weight of drill strings. To be capable of withstanding these extreme conditions, multiphase alloys with hard metals as skeleton material and tough, relatively soft metals as bonding agents are viable choices, and have been used in many other similar materials systems [44], such as tungsten (W) or WC combined with cobalt (Co), copper (Cu), manganese (Mn), and nickel (Ni). Other transition metals can provide a filling phase to assist with the sintering process. In this case, Cu is used to reduce porosity [45, 46]. This kind of low melting phase fills pores that appear during sintering [8].

In diamond-impregnated tools, matrices can be roughly divided into two groups: Co-based matrices and Co-free matrices [8]. The Co-free matrices can be subdivided into Cu-based, tinanium (Ti)-based, and iron (Fe)-based matrices [8]. One basic requirement

for a designed metal matrix is a low sintering temperature. A Cu-based matrix is a good choice for metal matrix composition, due to Cu's relatively low melting point of 1084.62 °C, compared with titanium (Ti, melting point is 1668 °C) and iron (Fe, melting point is 1538 °C). Another advantage of Cu-based matrices is that Cu does not appear to have a tendency to react or form stable compounds with carbon (C) [8]. On the other hand, the adhesion between Cu matrices and diamond particles is weak. In other words, there is little bonding in between [47].

The hardness of pure Fe is low and not suitable for diamond tools [48]. Iron must be alloyed with other metals, such as nickel, to increase hardness and transverse rupture strength. This research used the powder metallurgy method, which means that fine Fe powders (100–2500 nm in size) were necessary. However, compared with other materials that were used in this experiment, Fe powders were not convenient to store and process because of their easy oxidization.

Ti-based matrices are promising but have not been thoroughly studied [49]. Titanium is a carbide-former which can supply the bonding strength needed between matrix and diamond particles [8]. Similar to the Fe-based matrix, pure Ti is not capable of being a matrix for cutting tools. An additional hard phase metal needs to be added, such as Ni. Ni content helps increase matrix hardness; however, porosity will increase if the percentage of Ni is overly increased [8].

WC with Co content from 6 to 20 wt.% are widely used as matrix materials for various applications in which WC functions as an abrasion-resistant matrix, and cobalt

improves densification as well as diamond-retention properties. Powders of both materials are commercially available with wide particle size ranges.

In this work, the commonly used commercialized WC drill bit alloy with a Co composition of 10 and 16 wt.% were chosen as the starting DTM matrix of our work. WC alloys with a wide Co range from 16 to 36 wt.% were studied. In part of the samples, Cu was added to the WC-Co alloy as a densification assistant at the cost of reduced wear resistance.

Cobalt and its alloys have long been widely used as matrix materials for impregnated diamond tools [1]. Cobalt powder is commercially available in a variety of grades, such as particle size, size distribution, and chemical purity [1]. Cobalt powder can also cost-effectively attain nearly full theoretical density via hot pressing [1]. By using cobalt powder, especially in high temperature and high pressure processes, full density can be virtually achieved in relatively low temperature and pressure conditions [1]. Due to cobalt's combination of high yield strength and toughness, it also shows good diamond retention properties [1]. By adding the Cu element, the densification process of the matrix is assisted [73]. Although the wear resistance of the matrix is reduced, Cu is still an attractive choice [73]. Based on all of the above points, a fundamental composition for a DTM matrix is a combination of WC, Co and Cu.

Commercial diamond abrasives have been divided into two types, with those coarser than 80 U.S. mesh defined as saw grit, and those finer than 80 U.S. mesh defined as wheel abrasives [1]. The coarser saw grit was chosen for this work based on its

potential for faster ROP [74]. There are two ways to improve the bonding strength between diamonds and matrix, and increase the capacity of diamond-retention of the matrix: One is to roughen the diamond and matrix surface by chemical or thermal treatment, and the other is to take advantage of the carbide coating on the diamond surfaces [73]. Because the surface-roughening method suffers diamond graphitization or degradation [73], we chose using commercial synthetic diamonds supplied by Element Six Composites (Elbridge, NY, USA), with particle size ranging from 400 to 600 μm, and a TiC coating.

3.1.1 Influence of Different Diamond Volume Percentages

To study the influence of diamond volume percentage on the mechanical properties of DTM material, samples with diamond volume percentages ranging from 20–30 vol.% were prepared.

The volume percentage of diamonds cannot be controlled precisely as a result of limitations in the pellet-making process. Therefore, a special sample design search was conducted to find a set of samples with the ideal diamond volume percentage. To obtain this set of samples, the diamond grits were divided into two parts: an SD diamond group with particle sizes ranging from 400 μm to 500 μm, and a BD diamond group with particle sizes ranging from 500 to 600 μm. The pellets were also divided into two groups: a BP pellets group with a size of 1.0 to 1.18 mm in diameter, and a SP pellets group with a size of 0.9 to 1.0 mm in diameter. The sets of four samples were prepared by

combining the sizes of diamond grits and pellets in the way shown in Table 5. Matrix composition of these samples are WC with 36 wt.% Co.

3.1.2 Influence of Different Matrix Compositions

To study the influence of composition on mechanical properties, three sets of samples with different compositions were fabricated. Based on a previous study, small diamond sizes and small pellet sizes was selected for use in this part of the work.

In WC DTM materials, higher Co content leads to higher fracture toughness of the WC-Co system and avoids brittleness; thus a better matrix is achieved to hold the diamond grit. Enlarging the hard phase proportion increases matrix hardness and gives higher wear resistance. In this case, the worn-down rate of the matrix was reduced and the diamonds did not fall out of the matrix as quickly after the old DTM layer wore out. Therefore, the working time of abrasion for diamond particles was extended.

Based on this idea, three sets of samples were prepared, the compositions of which are shown in Table 6. The Set 1 samples have the matrix composition of 64 WC–36 Co, which means WC:Co = 1:1 in volume percentage. The Set 2 samples have the matrix composition of 84 WC–16 Co, which is close to the conventional WC-Co material. Set 3 samples with 6 wt.% Cu are designed to study the effect of Cu on matrix hardness and diamond bonding.

Please note that many of the tables in this section have acronyms that were introduced in Section 2. Rather than ask the reader to look up all of these acronyms, the

following is set forth as a review: Two groups of diamond were marked as BD (size range from 500 to 600 μm) and SD (size range from 400 to 500 μm). Pellets with sizes ranging from 0.9-1.0 mm in diameter (Group 6) were marked as SP, while those with sizes ranging from 1.0 to 1.18 mm (Group 7) were marked as BP. The qualified pellets (SP and BP) were collected, and the rest were pulled back into the rubber shaking bowl.

3.2 Experimental Results and Discussions

3.2.1 Physical Properties

3.2.1.1 Diamond Distribution

Optical scanning microscopy was used to study the diamond distributions on the vertical and horizontal cross sections of the DTM samples. Figures 18 and 19 provide examples of optical microscopy images obtained in this work. The shown sample has a matrix composition of WC at 36 wt.% Co, which is the same as the BD-BP, BD-SP, SD-BP, and SD-SP samples and a 30 vol.% diamond. Instead of using the pelletizing method, the green part of the shown sample was prepared by mixing raw materials on a rotor machine for 12 hours. The sample was then directly cold pressed and finally mROC compressed. Uniform diamond distribution could be observed on the microscopy images of this sample.

Similar optical microscopy studies were performed on the horizontal cross sections of the BD-BP, BD-SP, SD-BP and SD-SP samples. The microscopy images are shown in Figures 20 to 23. The diamond volume percentages were calculated based on these cross-

section images using the point-by-point method, and the results are shown in Table 7.

3.2.1.2 Density

The mROC samples were named as follows: 650-700-670A 1, where the first number (650) is the start current, the second number (700) is the midpoint current, and the third number (670) is the end current of the mROC process. Numbers 1 and 2 indicate the positions (upper and lower) of samples inside the graphite cell.

Table 8 shows the designed compositions of different sample sets. Using the diamond volume percentage obtained using the point-by-point method, the mROC compressed sample density can be estimated by this graphic method (shown in Table 9). The relative density (dense%) in this work was calculated using the sample density measured from the Archimedes method, divided by the density obtained from this graphic method. The relative density is a direct reference to the porosity or the sintering degree of the samples. The difference between the relative densities indicates the inconsistence between different trial samples with the same processing conditions. Results are shown in Tables 10 to 15.

3.2.1.3 Composition Change

During the pelletizing process, a considerable amount of matrix powder and diamond grits may stick onto the rubber bowl as a result of the sprayed binder liquid. For example, in an ideal situation 20 g of diamond grit and 440 g of matrix powders should produce 187.27 g SD-SP pellets with 272.73 g of the matrix powder left over. However,

in this work, less than 150 g of qualified SD-SP pellets could be obtained before all the powders were consumed.

In order to understand this effect on the composition of the final products, an energy dispersive x-ray spectroscopy (EDS) test was performed on one DTM insert with a matrix composition of 64WC-36Co. As shown in Fig. 24, the matrix part of this sample contains 65.92 wt.% W and 34.08 wt.% Co. Add C into consideration, and the real matrix composition of this sample is 67.32 WC–32.68 Co, in which the WC content is about 3 wt.% higher than the designed value. Therefore, the Co powders are more likely to stick onto the wall of the rubber bowl during pelletizing, which leads to slightly higher WC compositions inside the samples.

3.2.2 Mechanical Properties

3.2.2.1 Hardness

The Vickers hardness value was used in this work as a reference for the wear resistance property of the DTM insert. In order to minimize the effect of porosity, samples with the highest relative density were chosen from samples with the same processing conditions as those required for the Vickers Hardness Test. Five measurements were taken on each end of the sample and the final sample hardness is the average value of these 10 measurements.

Results of these hardness measurements are shown below. Based on Table 16, the Vickers hardness value of a DTM sample increases as the relative density increases,

which indicates the dependence of inert property on sintering. The Vickers hardness value also increases as the diamond volume percentage increases, as shown in Fig. 25. The only exception is the BD-SP sample with 34.10 vol.% of diamond. A possible explanation is the low relative densities of BD-SP inserts (92.07% and 92.34%) comparing to the SD-SP set.

Both relative density and diamond volume percentage show a direct proportional relationship with hardness. Comparing the results, an increase in relative density has more to do with the higher rate of hardness than an increase in diamond volume percentage. This indicates that the influence of relative density is greater than diamond volume percentage.

Table 17 shows the effect of matrix compositions on the Vickers Hardness values of DTM inserts. Comparing the SD-SP samples with 29.46 vol.% diamond grits, the Vickers hardness value increases as the WC composition in matrix increases (shown in Fig. 26). Therefore, adding hard materials like WC into the matrix can significantly increase the DTM matrix hardness, which leads to improvement in the wear-resistance of the inserts. The relative density of the SD-SP-Cu set is much smaller than the SD-SP or SD-SP-75WC sets, and has been excluded from this analysis.

To further study the effect of matrix composition on the Vickers hardness of DTM samples, the SD-SP-Cu combination was compared with the BD-SP samples, which have similar diamond volume percentages and relative densities. As shown in Table 18, although the SD-SP sample had 1% higher relative density, no significant difference

could be observed between the hardness of SD-SP-Cu and the BD-SP samples (seen from Fig. 27). This result indicates that adding Cu decreases matrix hardness.

3.2.2.2 Diamond Adhesion

In this work, all the diamond grits were coated with TiC to decrease diamond surface energy and improve the bonding formation between diamonds and the WC-Co matrix. Therefore, excellent diamond adhesion and retention can be expected in our DTM samples.

To study the effect of matrix composition on the diamond adhesion property, SD-SP, SD-SP-Cu and SD-SP-75WC samples were selected and SEM microstructure analysis of the fractured surfaces were performed. The SEM images are shown in Figures 28 to 33. The dark particles in the SEM images are actually diamond grits.

The matrices of the SD-SP-Cu samples show excellent diamond adhesion. The matrices were found to tightly adhere to diamond surfaces; some even covered the grit. The pits caused by shed diamonds with rough surfaces are further evidence of strong adhesion. The SD-SP sample matrix shows good adhesion as well, but not as good as the SD-SP-Cu set. The SD-SP-75W shows a smooth interfacial surface between the matrix and diamond grits, with a gap between the two materials. The pit surface was also smoother compared to the SD-SP-Cu sample. Based on these results, we can concur that softer matrix leads to better diamond adhesion properties and the addition of hard material results in a decrease in diamond retention.

To further study the effect of powder metallurgy processes on the diamond retention property of DTM materials, another set of samples was prepared with the same matrix material and a predebinding step was prepared. This set of samples was first debinding in a hydrogen atmosphere for 10.5 hours and then mROC compacted for 30 minutes. Figures 34 to 36 show the fractured surface microstructures of this set of samples.

Based on these figures, samples prepared with the predebinding step show superior diamond adhesion properties than direct mROC compaction samples. However, the addition of this predebinding step increased the complexity and cost of the process.

3.2.3 Microstructure

The microstructures and phase distributions of DTM samples were studied on the 64WC-36Co, 84WC-16Co, and 64WC-30Co-Cu samples. As shown in Figures 37 to 45, SEM images were taken on the polished sample surface with magnifications of 1000x, 10000x, and 30000x. The darker areas on the SEM image indicate phases containing mainly low atomic number elements like Co or Cu, and the lighter areas refer to WC.

As the figures show, the polished surfaces show a homogeneous structure at 1000x magnification with some small pores. These pores are likely formed by vaporization or carbonization of binder wax during the mROC process. The WC and Co/Cu phase separation begins to be observable with 10000x magnification and a homogeneous dispersion of Co/Cu in the WC matrix could be observed. The dimensions of Co/Cu and WC phases are measured at 30000x magnification. The SEM images show almost fully

dense microstructures with limited pore formation, which indicates excellent solid state sintering of DTM materials during the mROC process.

Fig. 18: Plot shows the vertical cross-section of DTM insert.

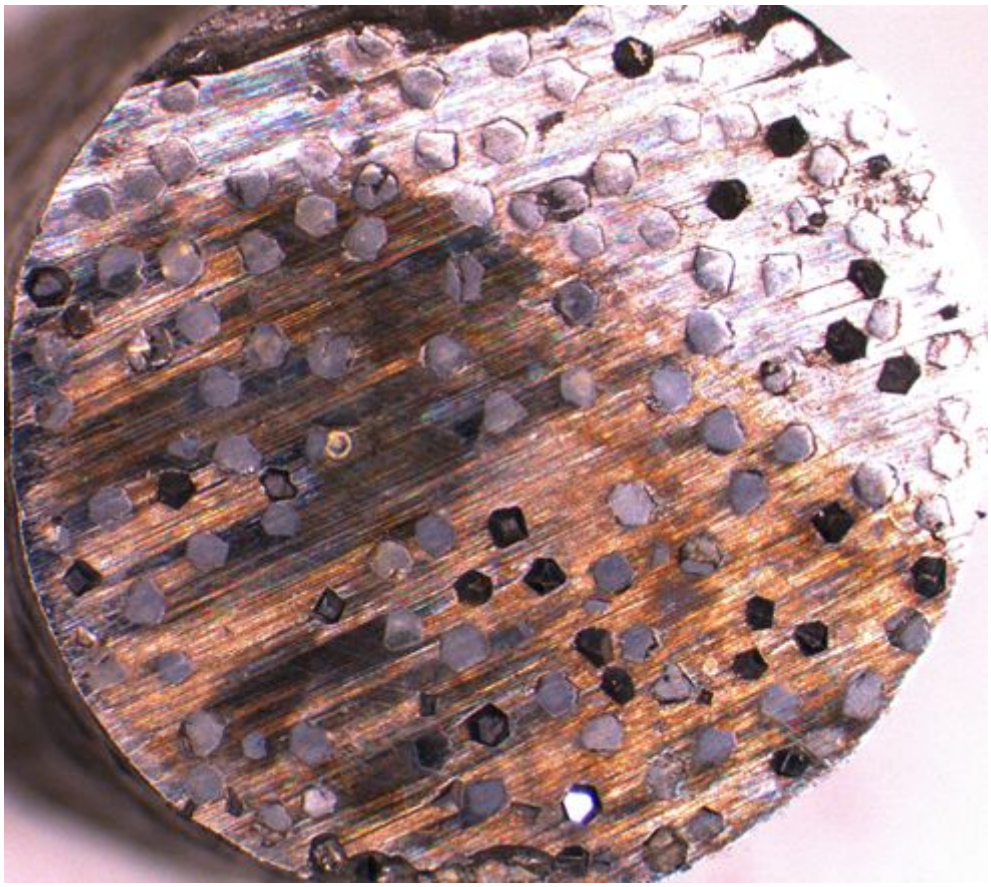

Fig. 19: Photo shows the horizontal cross-section of insert made without pellet-making method.

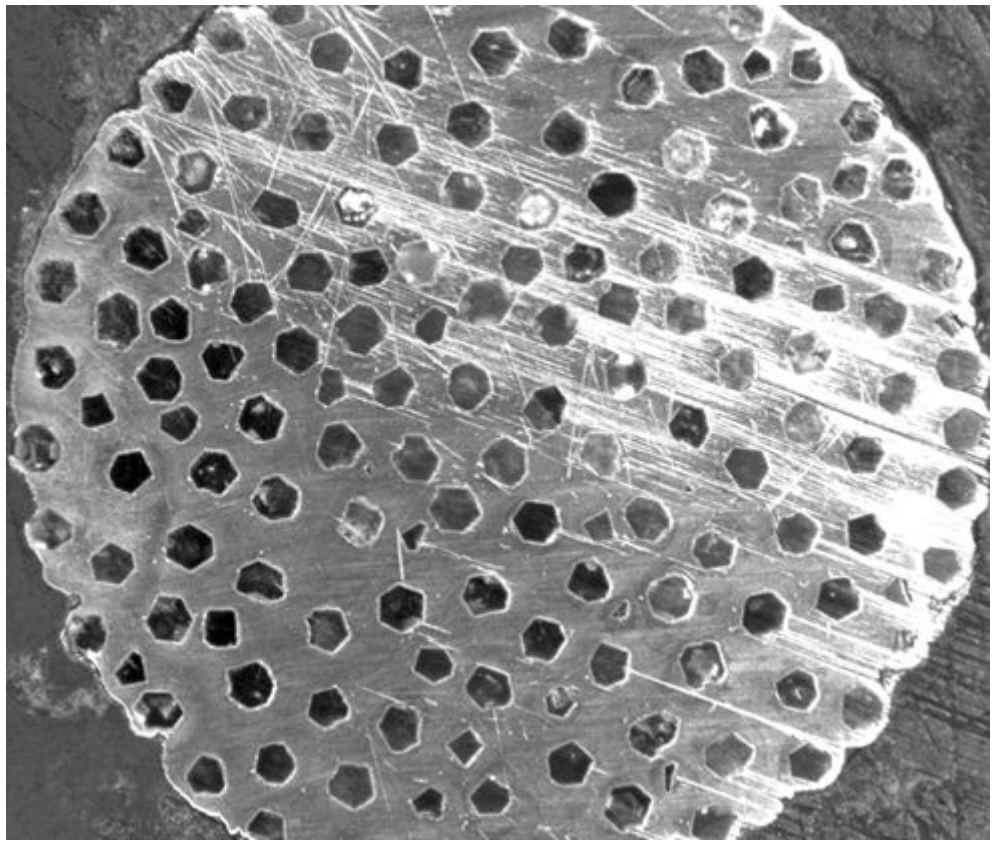

Fig. 20: Photo shows the horizontal cross-section of a BD-BP DTM insert.

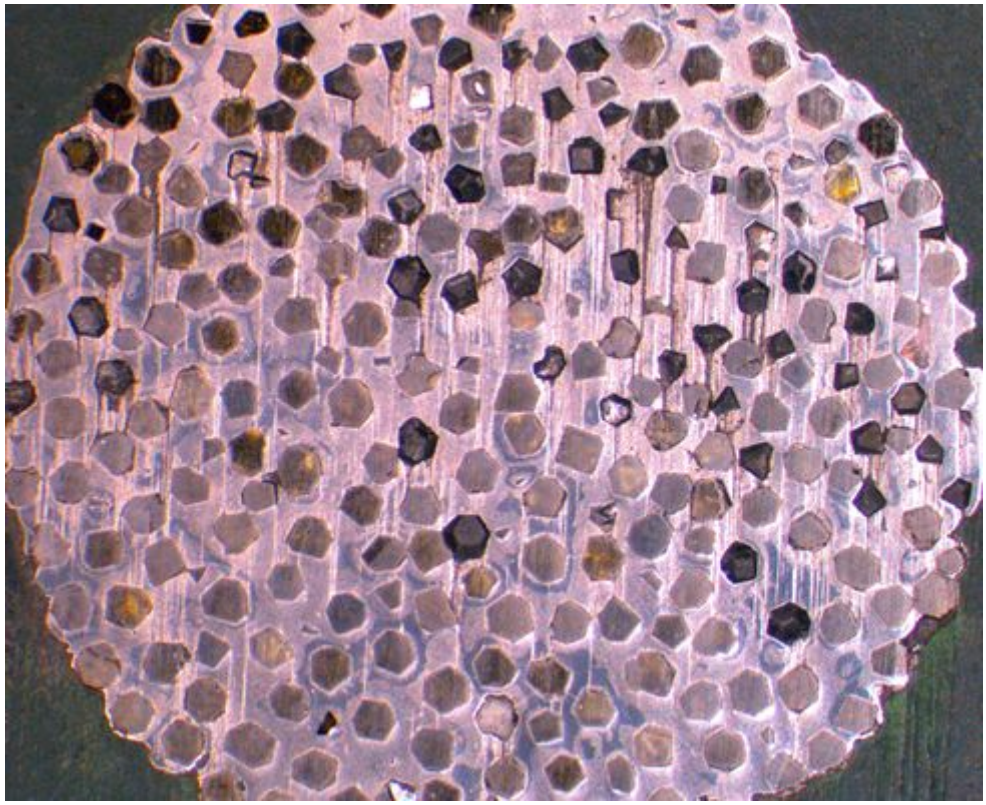

Fig. 21: Photo shows the horizontal cross-section of a BD-SP DTM insert.

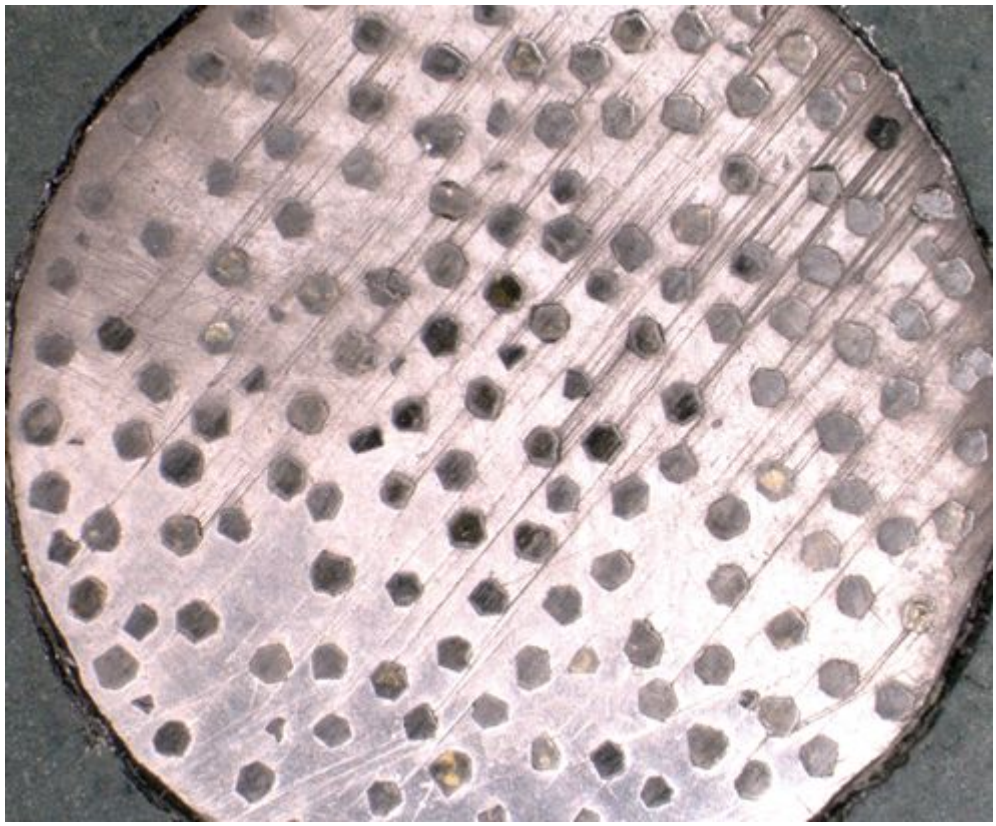

Fig. 22: Photo shows the horizontal cross-section of an SD-BP DTM insert.

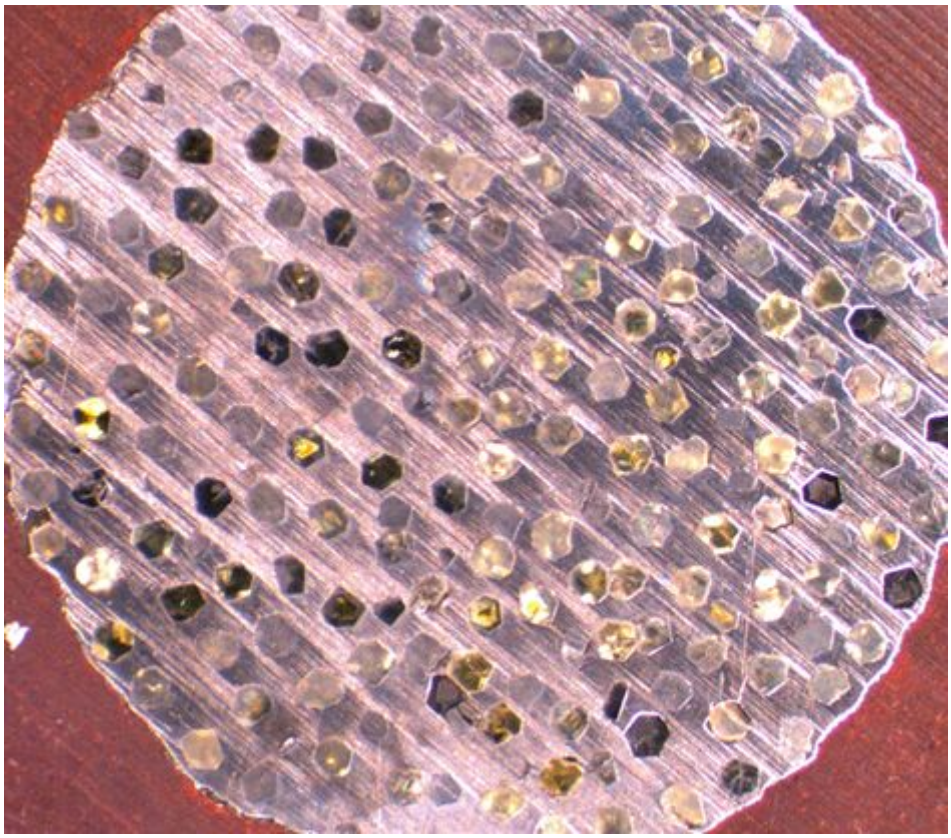

Fig. 23: Photo shows the horizontal cross-section of an SD-SP STM insert.

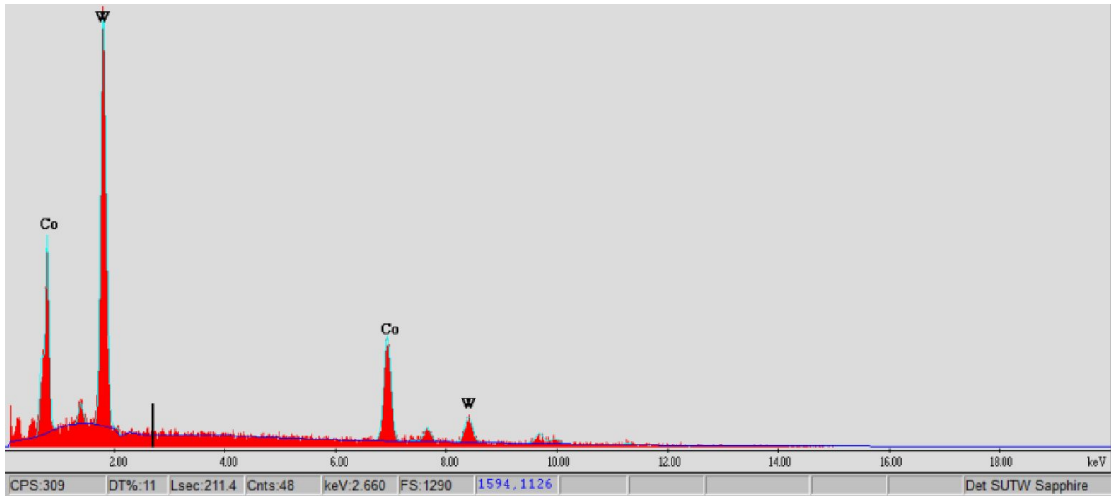

Fig. 24: EDS result calculates the composition of 64 WC-36 Co matrix.

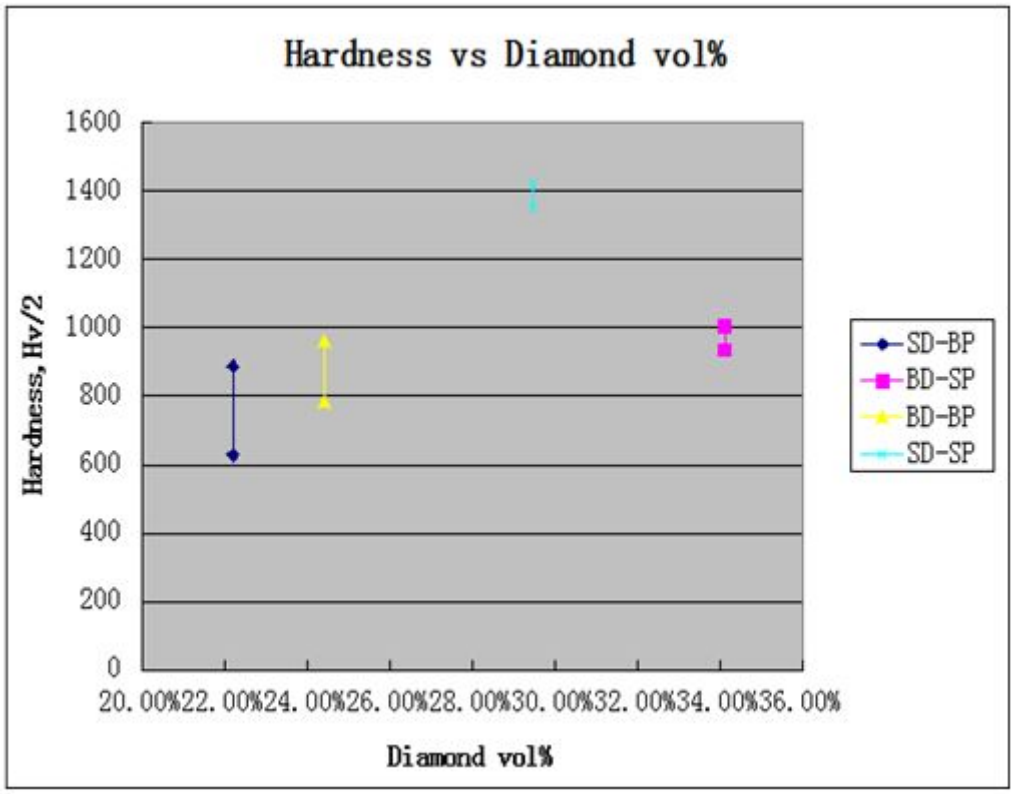

Fig. 25: Plot showing the Vickers Hardness of the matrix versus diamond volume percent for DTM samples tested.

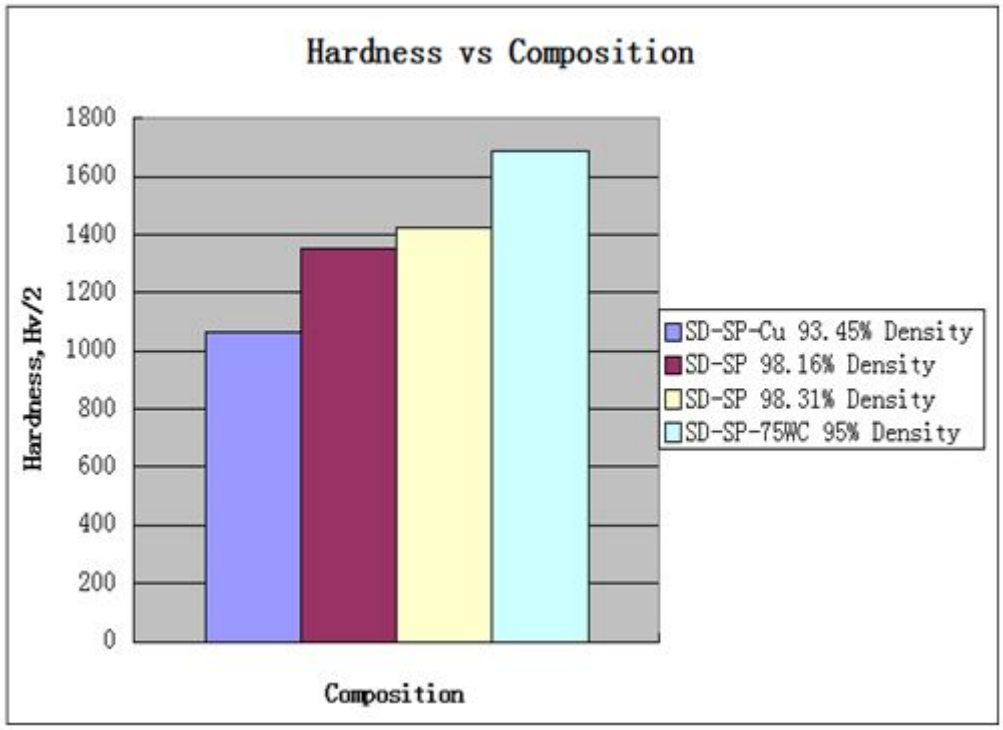

Fig. 26: Plot showing the Vickers Hardness of the matrix versus matrix composition for DTM samples tested.

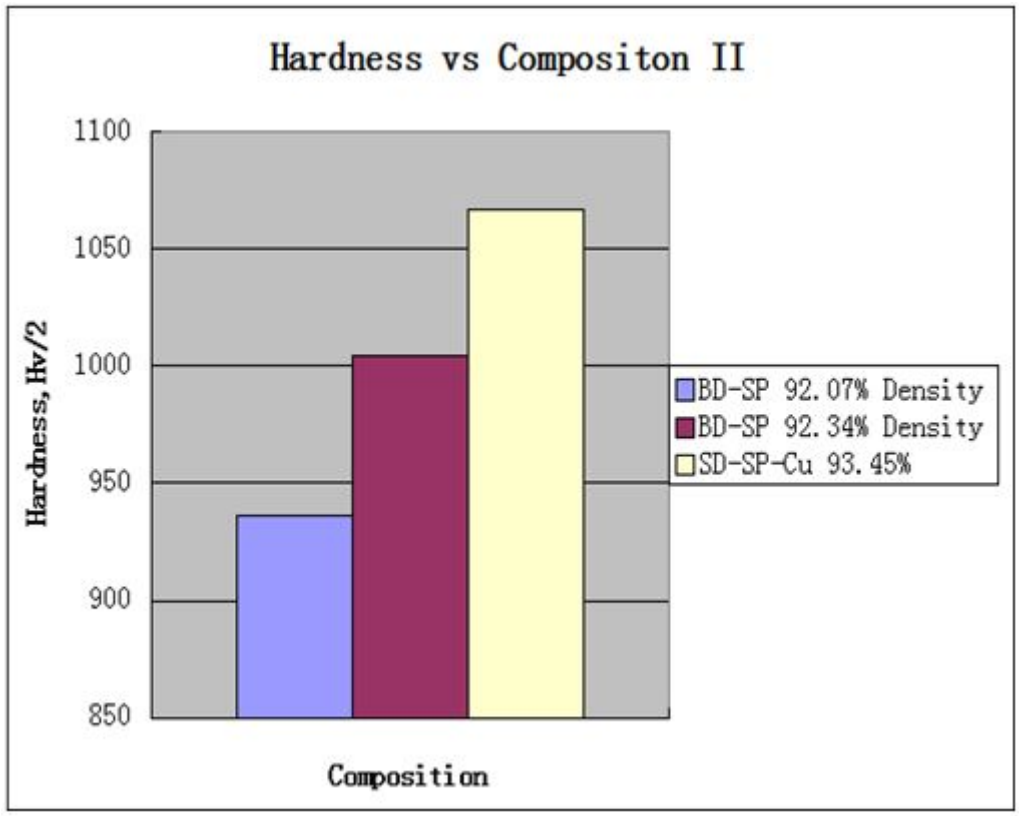

Fig. 27: Plot shows the Vickers Hardness of the matrix versus matrix composition for DTM samples tested II.

Fig. 28: Photo shows contact between SD-SP-Cu matrix and diamond grit with great diamond adhesion I.

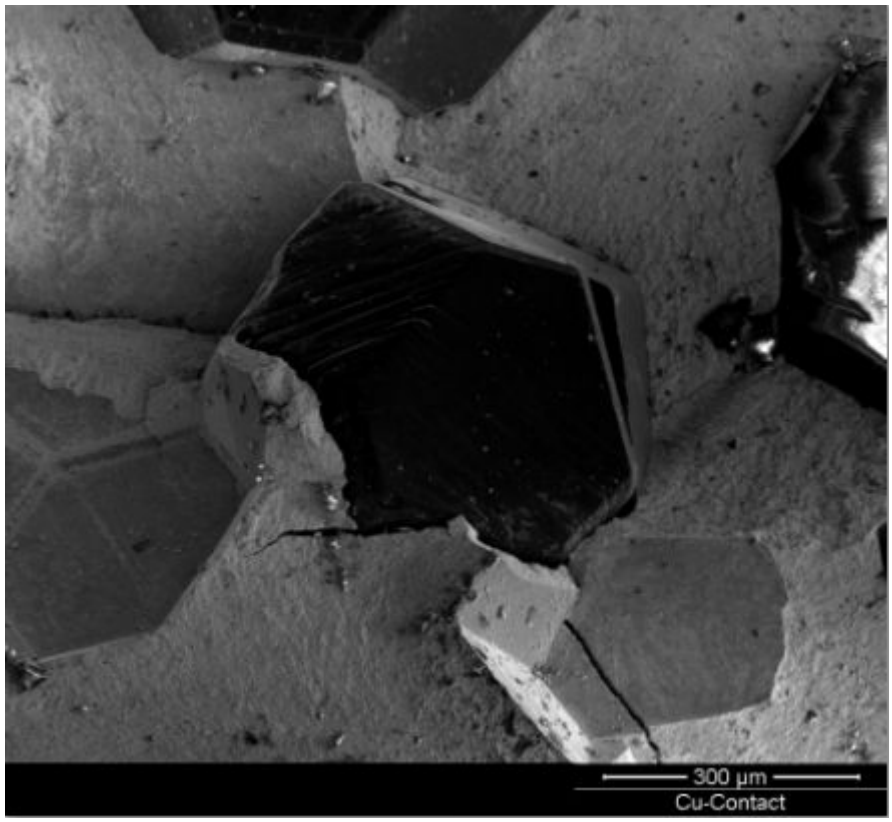

Fig. 29: Photo shows contact between SD-SP-Cu matrix and diamond grit with great diamond adhesion II.

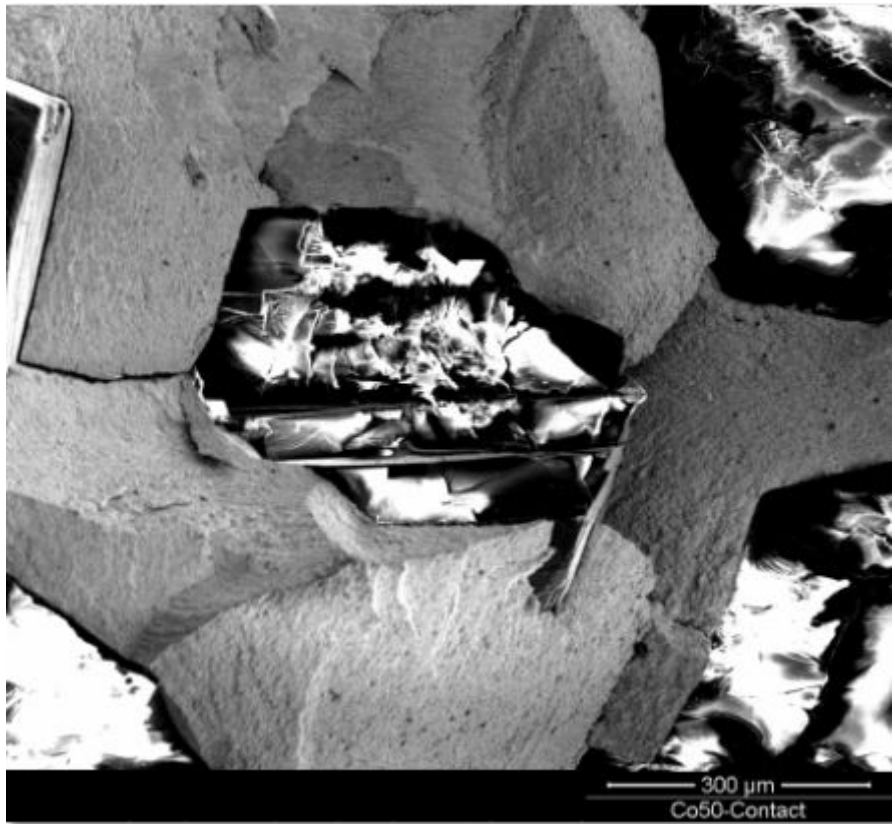

Fig. 30: Photo shows contact between SD-SP matrix and diamond grit with good diamond adhesion I.

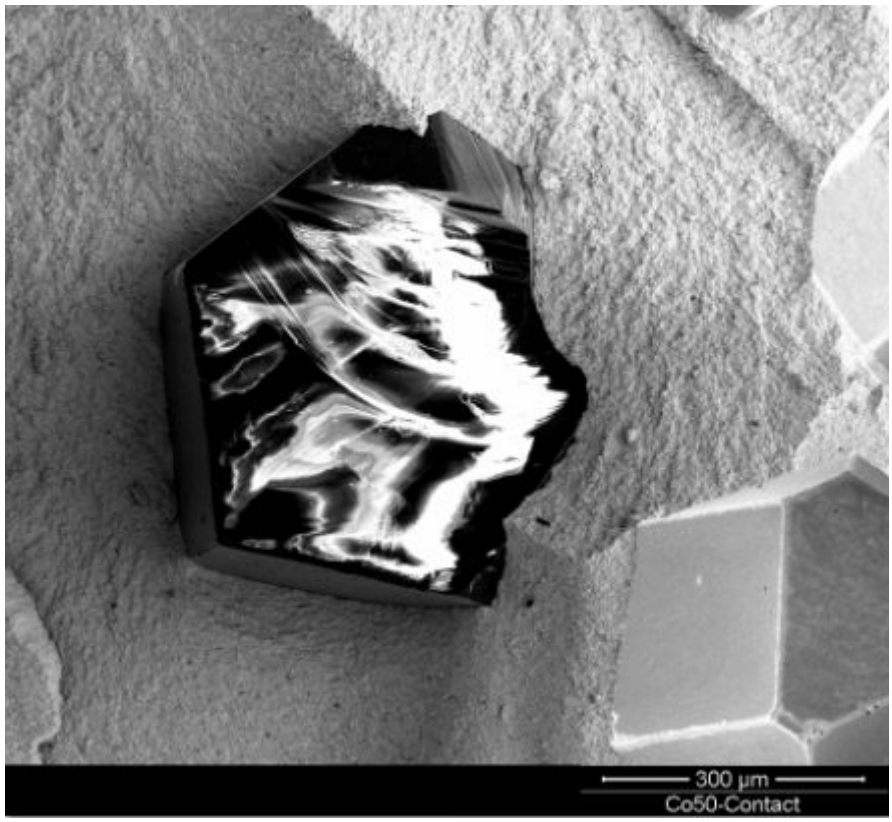

Fig. 31: Photo shows contact between SD-SP matrix and diamond grit with good diamond adhesion II.

Fig. 32: Photo shows contact between SD-SP-75WC matrix and diamond grit with poor diamond adhesion I.

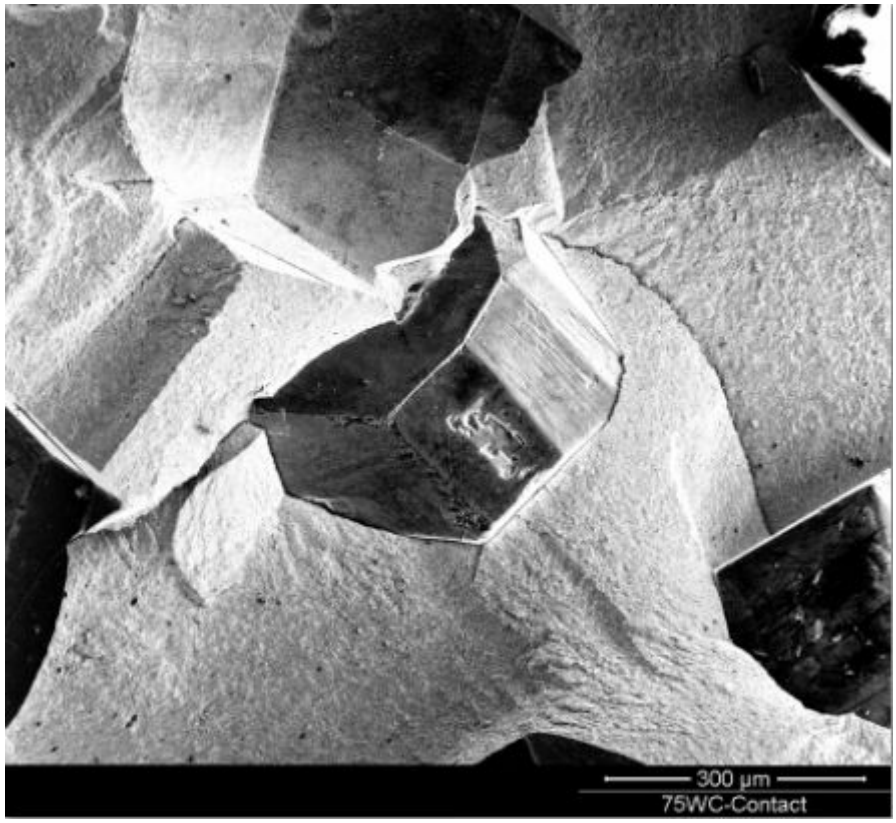

Fig. 33: Photo shows contact between SD-SP-75WC matrix and diamond grit with poor diamond adhesion II.

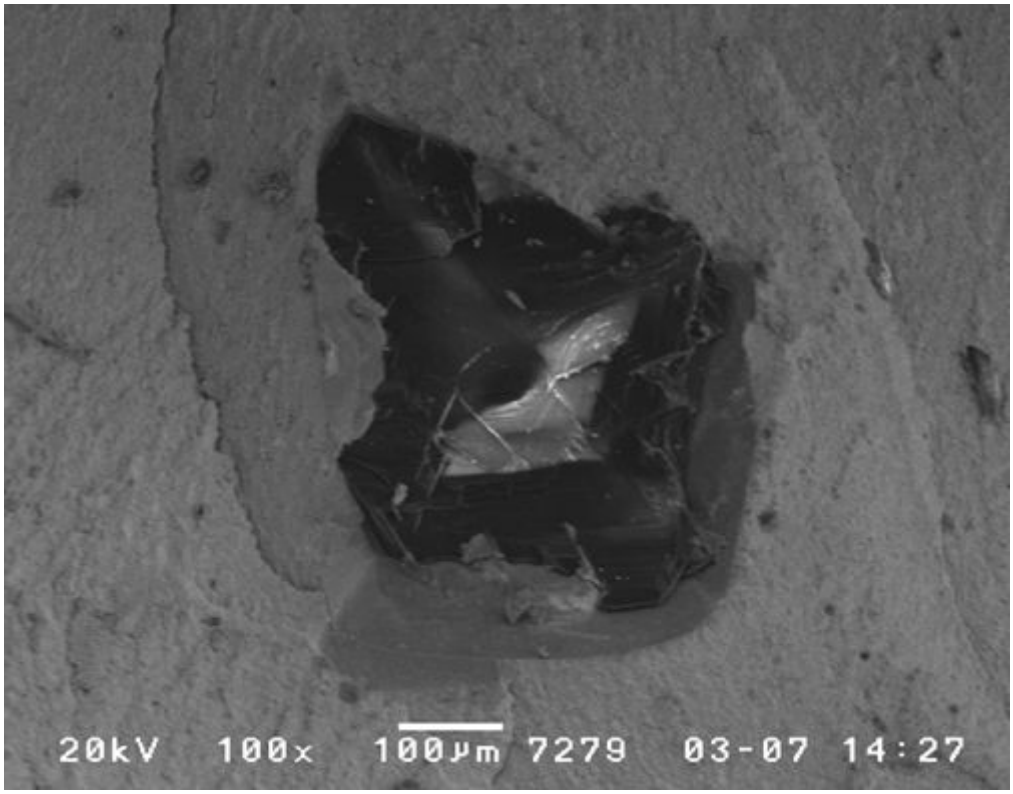

Fig. 34: Plot shows the diamond adhesion between diamond and matrix formed by process with a separate debinding step in the presence of hydrogen for 10.5 hours I.

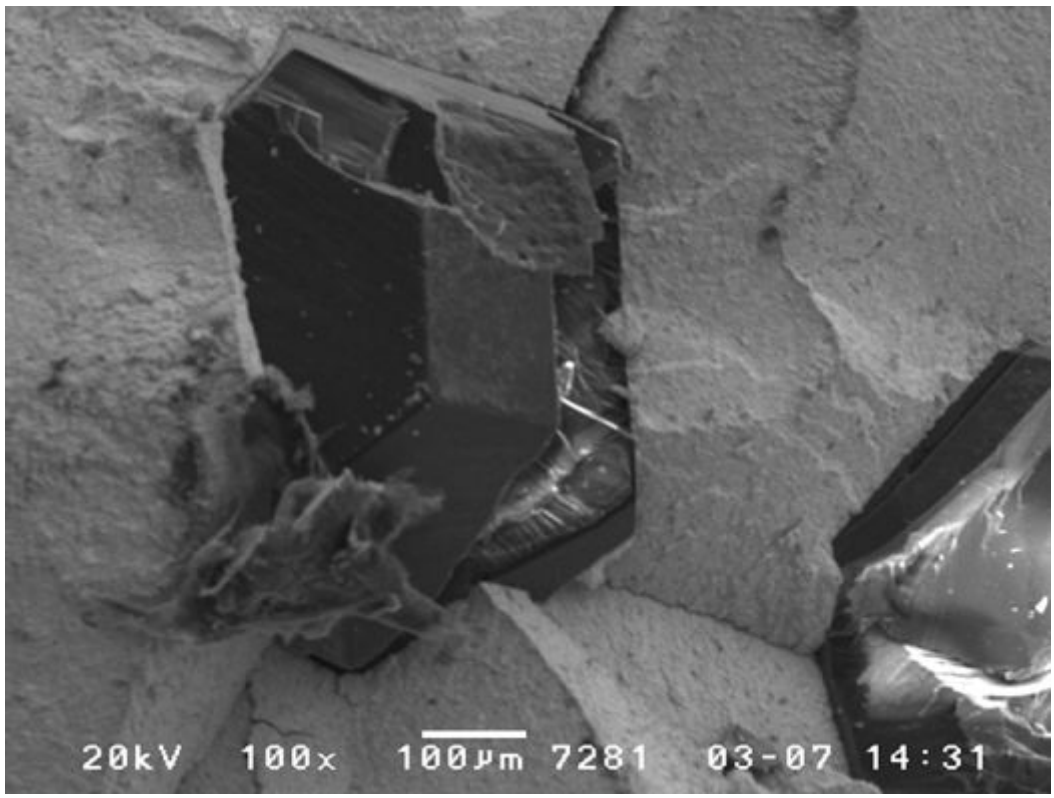

Fig. 35: Plot shows the diamond adhesion between diamond and matrix formed by process with a separate debinding step in the presence of hydrogen for 10.5 hours II.

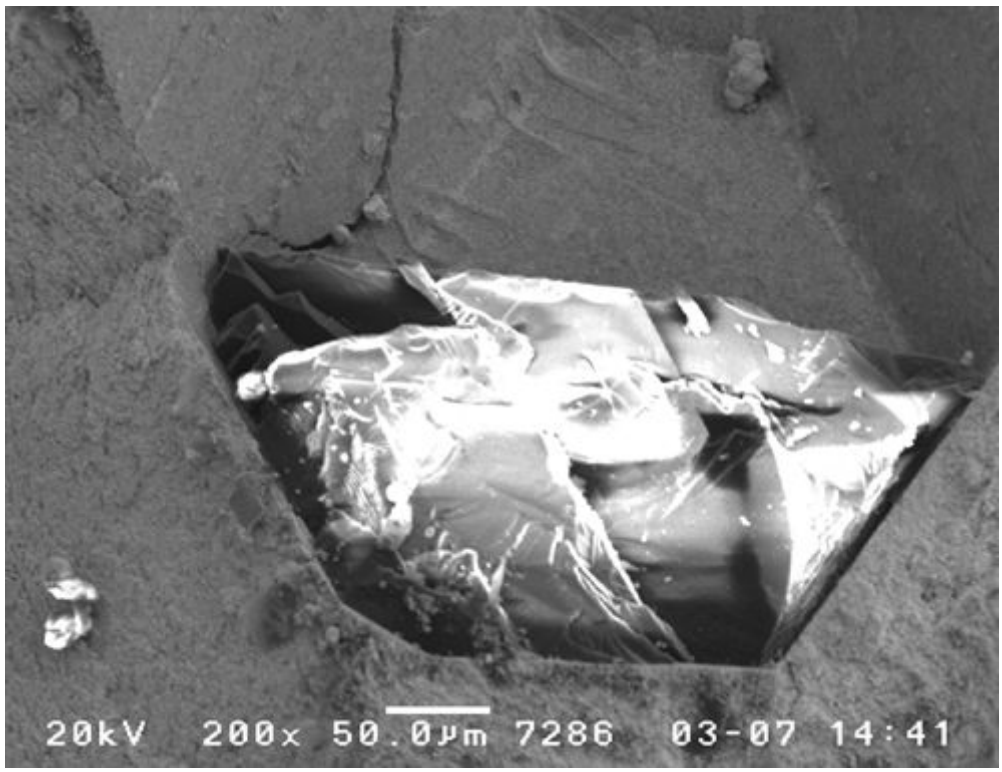

Fig. 36: Plot shows the diamond adhesion between diamond and matrix formed by process with a separate debinding step in the presence of hydrogen for 10.5 hours III.

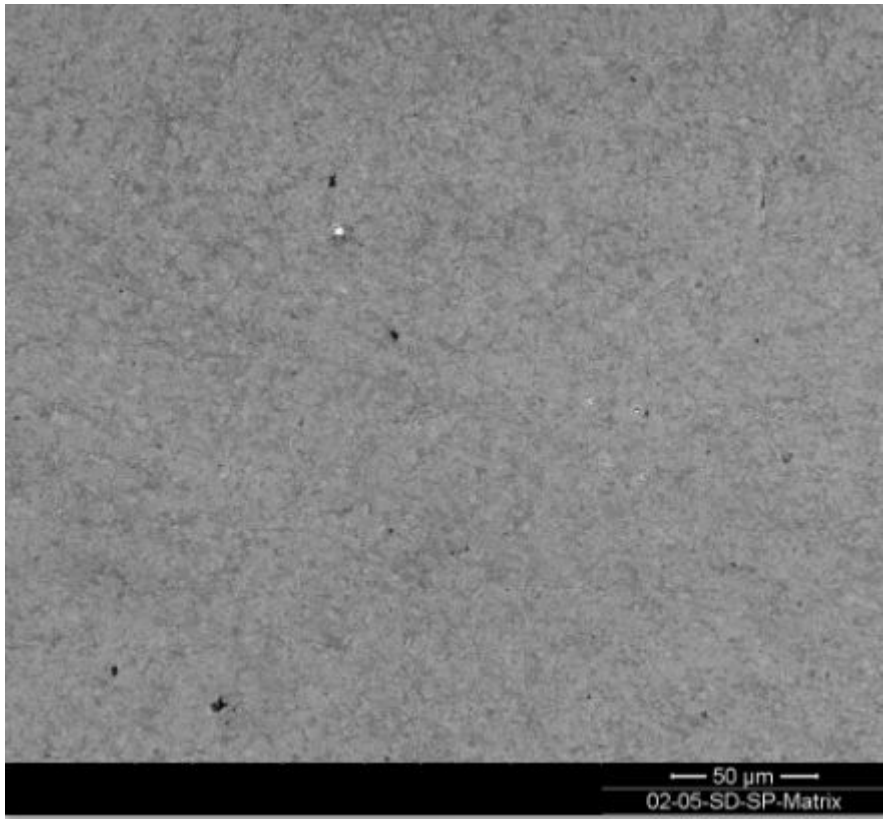

Fig. 37: SEM micrograph of 64 WC–36 Co matrix under 1,000x magnification.

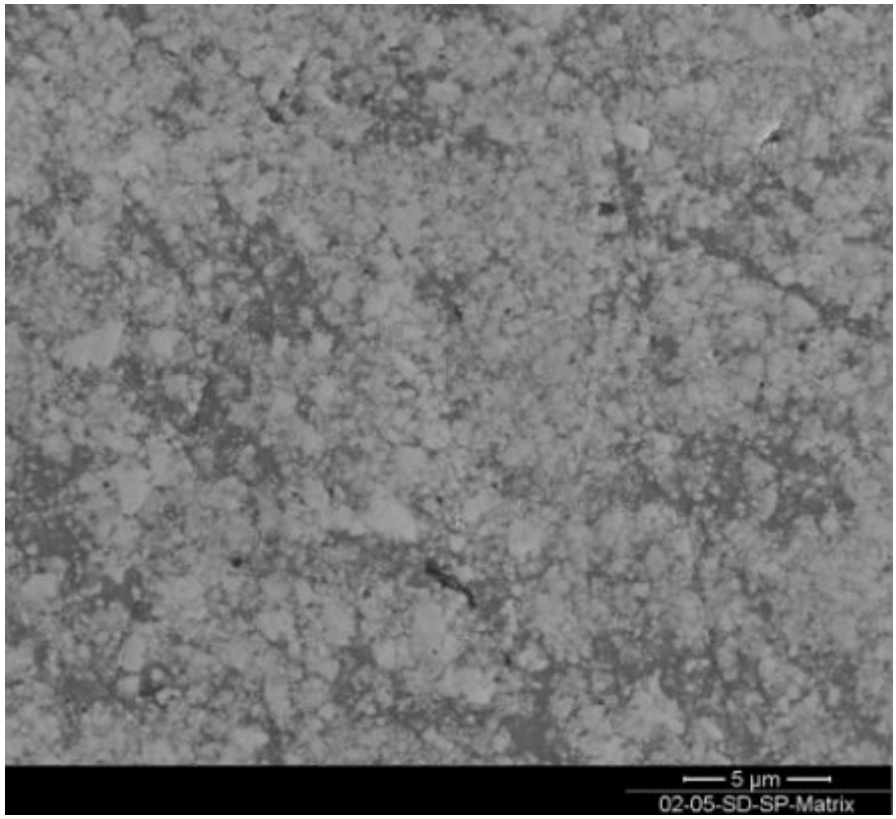

Fig. 38: SEM micrograph of 64 WC–36 Co matrix under 10,000x magnification.

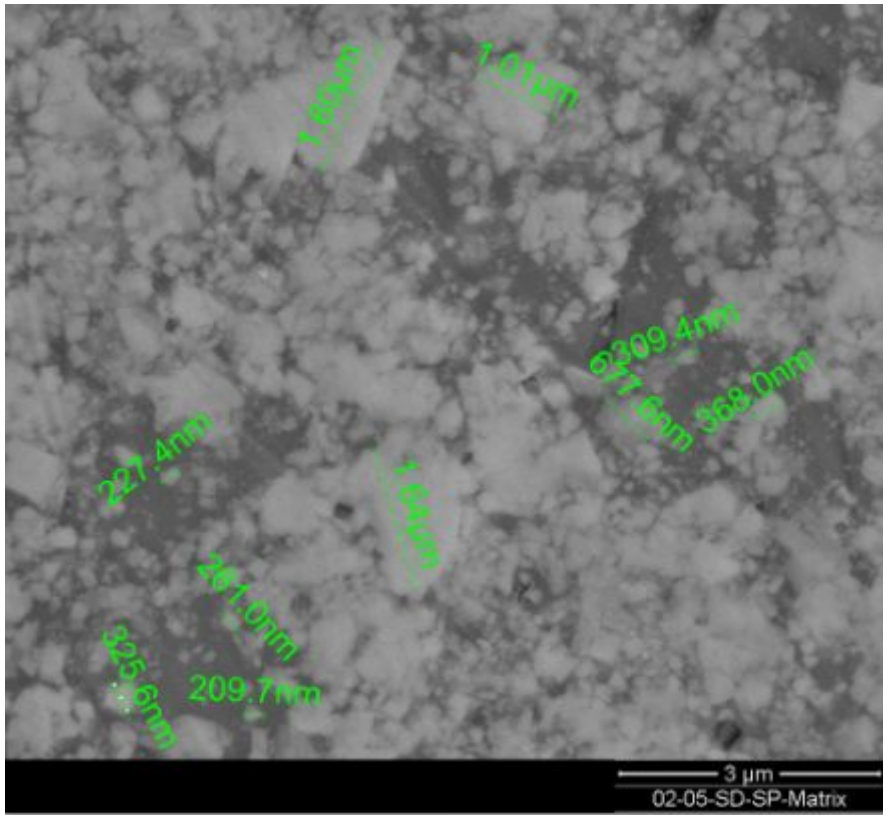

Fig. 39: SEM micrograph of 64 WC–36 Co matrix under 30,000x magnification.

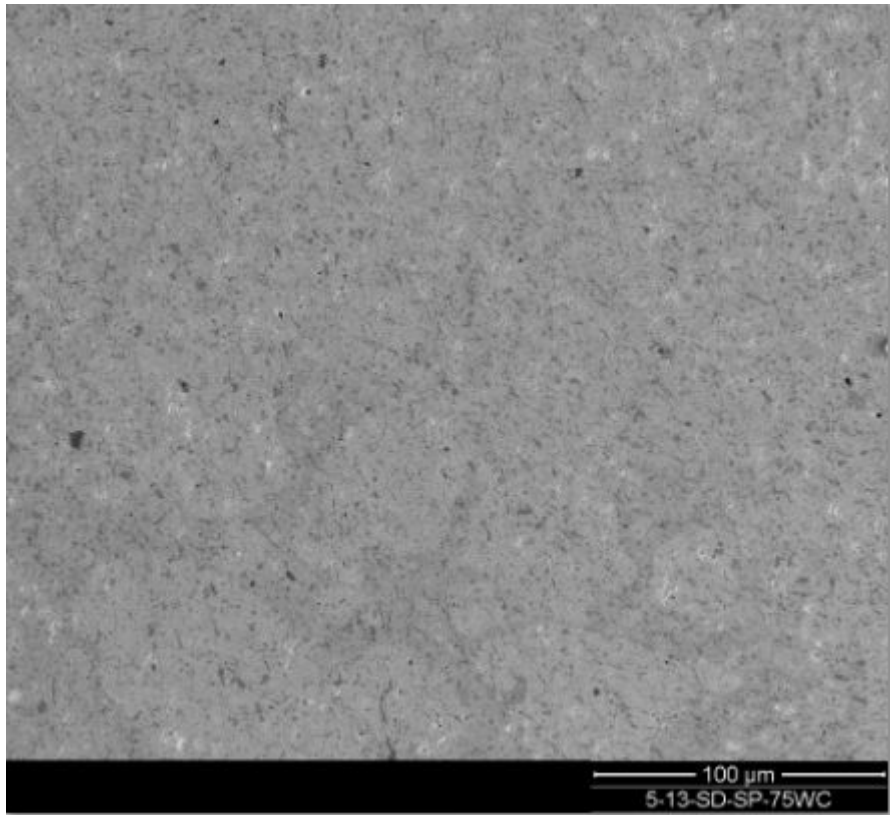

Fig. 40: SEM micrograph of 84 WC–16 Co matrix under 1,000x magnification.

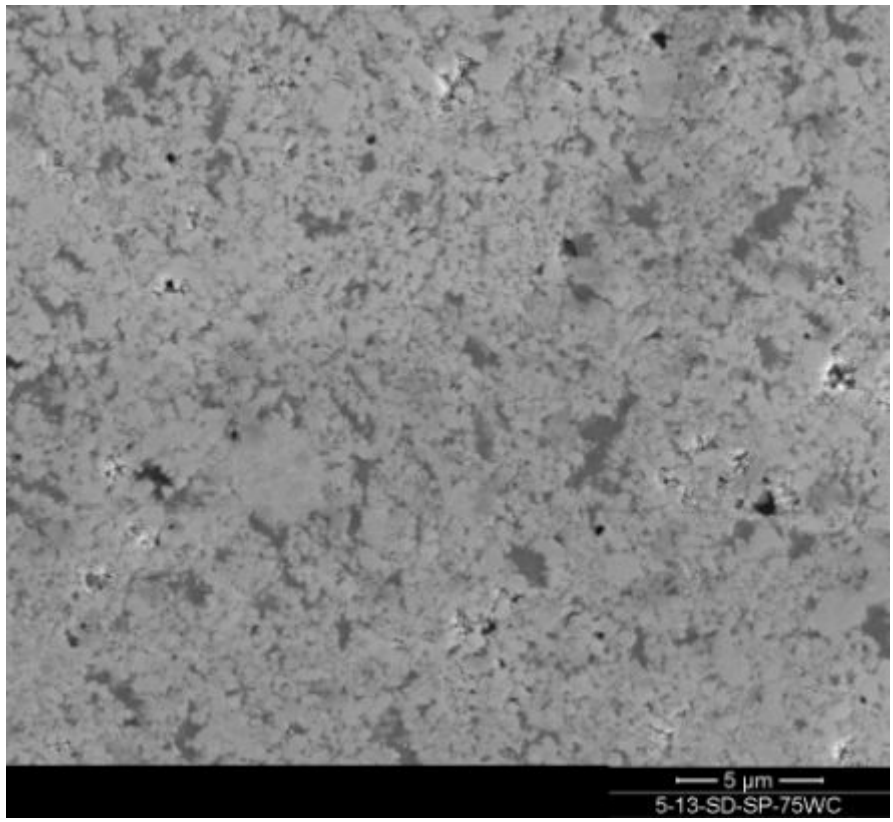

Fig. 41: SEM micrograph of 84 WC–16 Co matrix under 10,000x magnification.

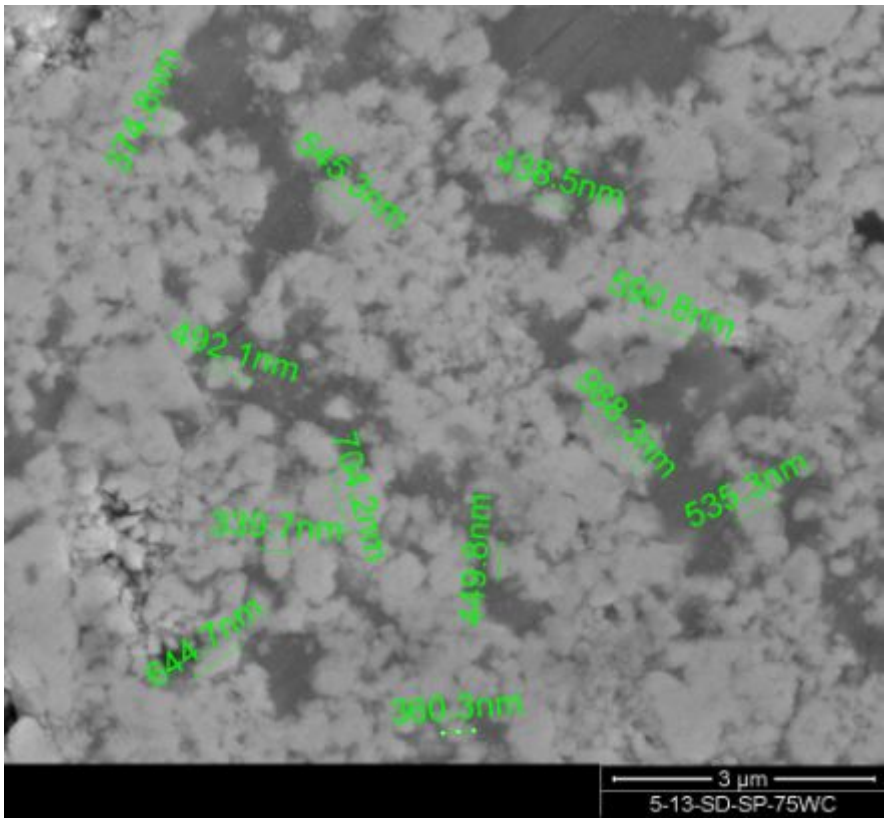

Fig. 42: SEM micrograph of 84 WC–16 Co matrix under 30,000x magnification.

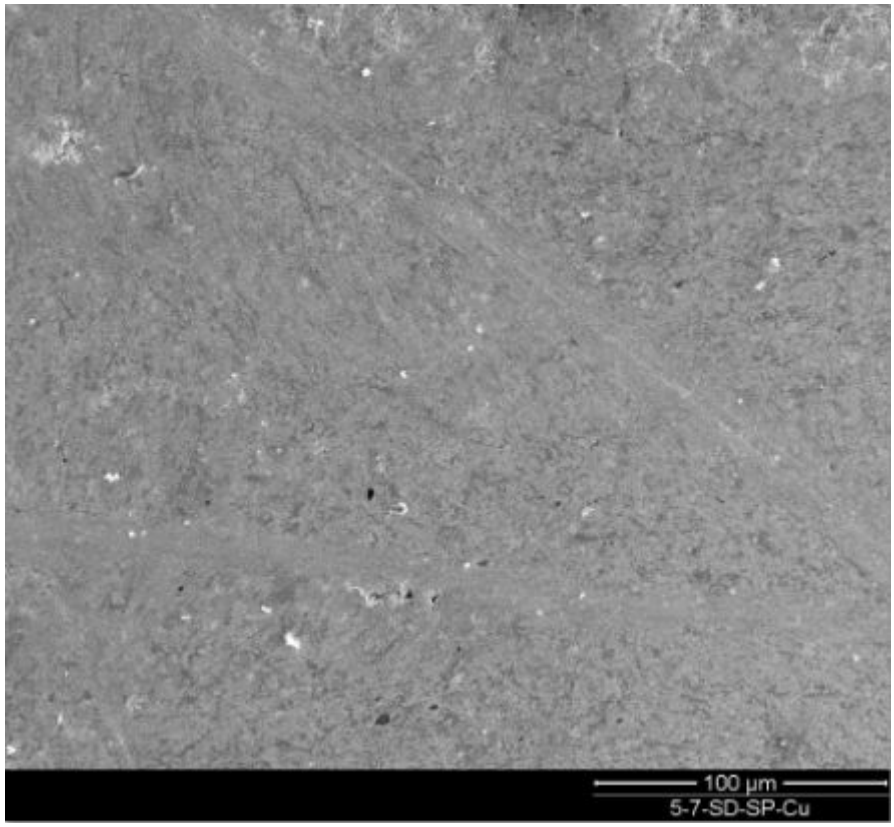

Fig. 43: SEM micrograph of 64 WC-30 Co-Cu matrix under 1,000x magnification.

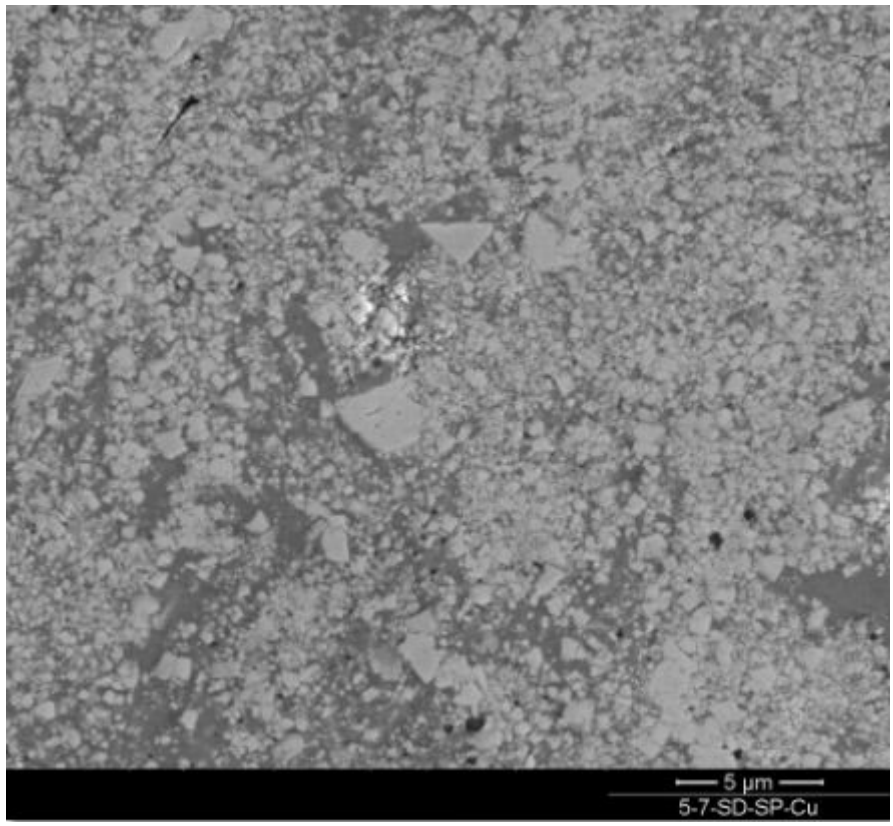

Fig. 44: SEM micrograph of 64 WC–30 Co–Cu matrix under 10,000x magnification.

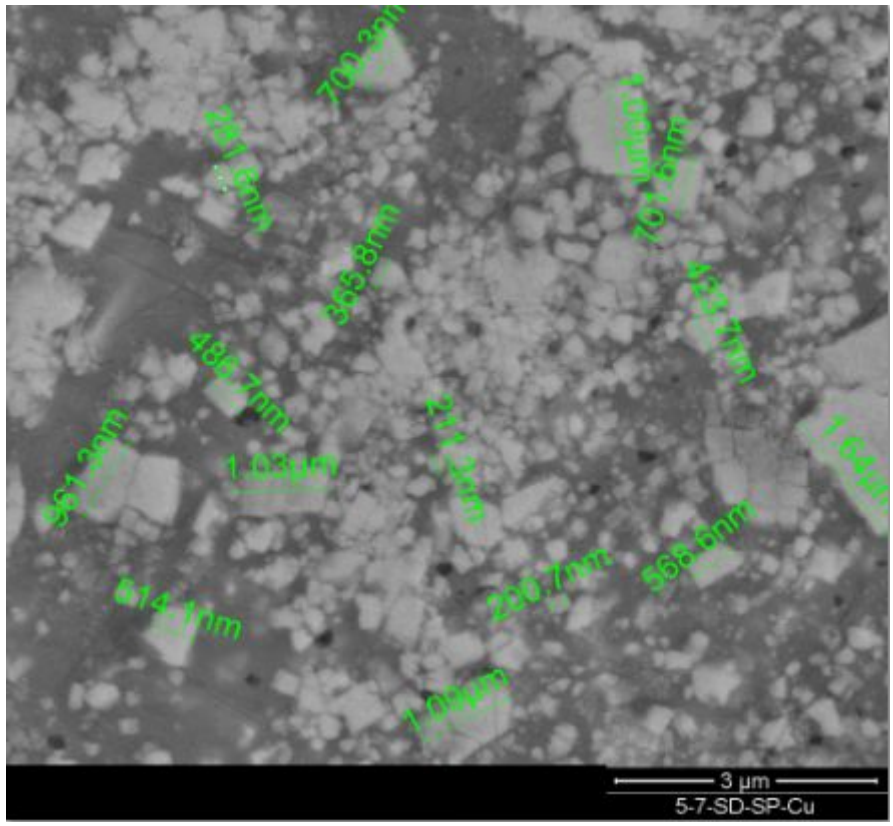

Fig. 45: SEM micrograph of 64 WC–30 Co–Cu matrix under 30,000x magnification.

Table 5: Four Sets of diamond/pellet sizes

Set	Diamond Size, μm	Pellet Size, mm
BD-SP	500-600	0.9-1.0
SD-SP	400-500	0.9-1.0
BD-BP	500-600	1.0-1.18
SD-BP	400-500	1.0-1.1

Table 6: Three Sets of matrix compositions

Set	Composition, by wt%
SD-SP	64WC-36Co
SD-SP-75WC	84WC-16Co
SD-SP-Cu	64WC-30Co-6Cu

Table 7: Relationship between diamond/pellet size and diamond volume percentage

Set	Diamond vol.%
BD-SP	34.10%
SD-SP	29.46%
BD-BP	24.40%
SD-BP	22.20%
SD-SP-Cu	Same as SD-SP
SD-SP-75WC	Same as SD-SP

Table 8: Designed compositions

Set	WC, wt%	Co, wt%	Diamond, wt%	Cu, wt%
BD-BP	58.42%	33.12%	8.46%	0%
BD-SP	55.59%	31.51%	12.90%	0%
SD-BP	59.00%	33.45%	7.55%	0%
SD-SP	57.01%	32.32%	10.68%	0%
SD-SP-Cu	57.01%	26.93%	10.68%	5.39%
SD-SP-75WC	76.11%	14.38%	9.50%	0%

Table 9: Graphic theoretical density

	Graphic Theoretical Density, g/cm^3
BD-BP	10.158
BD-SP	9.315
SD-BP	10.351
SD-SP	9.713
SD-SP-Cu	9.713
SD-SP-75WC	10.913

Table 10: Density, relative density and similarity of two samples in one trial of compaction for the BD-BP Group

BD-BP	Density, g/cm^3	dense%	similarity
690A 1	9.609	0.945953928	single insert
660A 1	9.69	0.953927939	0.989164087
660A 2	9.585	0.943591258	
730A 1	10.028	0.987202205	0.989030714
730A 2	9.918	0.976373302	
745A 1	10	0.984445757	0.9484
745A 2	9.484	0.933648356	
average BD-BP	**9.759142857**	0.960734678	
theoretical	**10.158**		

Table 11: Density, relative density and similarity of the two samples in one trial of compaction for the BD-SP Group

BD-SP	Density, g/cm^3	dense%	similarity
715-610A 1	8.602	0.92345679	0.996977447
715-610A 2	8.576	0.920665593	
700-570A 1	8.128	0.872571122	0.976101837
700-570A 2	8.327	0.893934514	
690-610A 1	8.465	0.908749329	0.904548139
690-610A 2	7.657	0.822007515	
715-620A 1	8.478	0.910144928	0.955414013
715-620A 2	8.1	0.869565217	
average BD-SP	**8.291625**	0.890136876	
theoretical	**9.315**		

Table 12: Density, relative density and similarity of the two samples in one trial of compaction for the SD-BP Group

SD-BP	Density, g/cm^3	dense%	similarity
600-550A 1	9.609	0.928316105	0.991640867
600-550A 2	9.69	0.936141436	
670-595A 1	9.629	0.930248285	0.972790529
670-595A 2	9.367	0.904936721	
600-590A 1	9.688	0.935948218	0.986787779
600-590A 2	9.56	0.923582263	
680-600A 1	9.809	0.947637909	0.968396371
680-600A 2	9.499	0.917689112	
average SD-BP	**9.606375**	0.928062506	
theoretical	**10.351**		

Table 13: Density, relative density and similarity of the two samples in one trial of compaction for the SD-SP Group

SD-SP	Density, g/cm^3	dense%	similarity
710-635A 1	9.546	0.982806548	0.998533417
710-635A 2	9.532	0.981365181	
725-640A 1	9.055	0.93225574	0.987997818
725-640A 2	9.165	0.943580768	
750-680A 1	9.43	0.970863791	0.995440085
750-680A 2	9.387	0.966436734	
690-615A 1	9.128	0.93977144	0.965108903
690-615A 2	9.458	0.973746525	
average SD-SP	**9.337625**	0.961353341	
theoretical	**9.713**		

Table 14: Density, relative density and similarity of the two samples in one trial of compaction for the SD-SP-Cu Group

SD-SP-Cu	Density, g/cm^3	dense%	similarity
540-535A 1	8.81	0.907031813	0.986341245
540-535A 2	8.932	0.919592299	
650-600A 1	8.723	0.898074745	0.965253956
650-600A 2	9.037	0.930402553	
745-635A 1	8.881	0.914341604	0.994847093
745-635A 2	8.927	0.919077525	
790-870-690A 1	9.074	0.934211881	0.97079568
790-870-690A 2	8.809	0.906928858	
average SD-SP-Cu	**8.899125**	0.91620766	
theoretical	**9.713**		

Table 15: Density, relative density and similarity of the two samples in one trial of compaction for the SD-SP-75WC Group

SD-SP-75WC	Density, g/cm3	dense%	similarity
700-730-625A 1	9.646	0.883899936	0.952409163
700-730-625A 2	10.128	0.928067442	
750-650A 1	10.194	0.934115275	0.989111242
750-650A 2	10.083	0.92394392	
730-530A 1	10.365	0.94978466	single insert
average SD-SP-75WC	**10.0832**	0.923962247	
theoretical	**10.913**		

Table 16: Results of Vickers Hardness Test for matrix based on diamond volume percentage influence

Sample	Set	Diamond vol.%	Density, g/cm3	%Density	Average hardness, Hv/2
680-600A 2	SD-BP	22.20%	9.499	91.77%	629.54
715-610A 2	BD-SP	34.10%	8.576	92.07%	935.81
715-610A 1	BD-SP	34.10%	8.602	92.34%	1004.58
680-600A 1	SD-BP	22.20%	9.809	94.77%	886.94
730A 2	BD-BP	24.40%	9.918	97.71%	782.78
710-635A 2	SD-SP	29.46%	9.532	98.16%	1349.19
710-635A 1	SD-SP	29.46%	9.546	98.31%	1425.83
730A 1	BD-BP	24.40%	10.028	98.80%	958.92

Table 17: Results of Vickers Hardness of matrix for the study of matrix composition influence

Sample	Set	Composition	%Density	average Hv/2
790-870-690A 1	SD-SP-Cu	64WC-30Co-6 Cu	93.45%	1066.85
710-635A 2	SD-SP	64WC-36Co	98.16%	1349.19
710-635A 1	SD-SP	64WC-36Co	98.31%	1425.83
730-530A 1	SD-SP-75WC	84WC-16Co	95%	1685.26

Table 18: Results of Vickers Hardness of matrix for the study of Cu content influence

Sample	Set	Diamond vol.%	%Density	average Hv/2
715-610A 2	BD-SP	34.10%	92.07%	935.81
715-610A 1	BD-SP	34.10%	92.34%	1004.58
790-870-690A 1	SD-SP-Cu	29.46%	93.45%	1066.85

CONCLUSION

1) A process was successfully developed for making diamond-tungsten-metal (DTM) composite for rock-drilling applications, including the processes for granulation of composite powder of WC/Co-coated diamond grit and the modified rapid omnidirectional compaction process for consolidation of the composite materials.

2) An increase in diamond volume percentage in the composite increased the hardness of the matrix.

3) Relative density had a greater influence on changing matrix hardness than diamond volume percentage.

4) By adding more WC content (hard phase within the matrix), matrix hardness was increased, but additionally, the adhesion between the matrix and diamond grit was decreased.

5) Cu content was seen to improve diamond adhesion, but decrease matrix hardness.

6) Using a high-temperature, high-pressure forming process with a separate debinding step in the presence of hydrogen gave better diamond adhesion than when the debinding was performed in conjunction with rapid-heating omnidirectional compaction (mROC), although the latter was performed in a much shorter time.

REFERENCES

[1] Konstanty J. *Powder Metallurgy Diamond Tools*; Elsevier: Amsterdam, 2005; pp 2-87.

[2] Fang Z.; Griffo A.; White B.; Lockwood G.; Belnap D.; Hilmas G.; and Bitler J.. Fracture Resistance Super Hard Materials and Hard Metals Composite With Functionally Designed Microstructure. *Intl. J., Refractory Metals & Hard Matls.*. **2001,** 19, pp 453-459.

[3] Fang Z.; Lockwood G.; and Griffo A.. A Dual Composite of WC-Co. *Metallurgical And Materials Transactions A*, **1999,** 12, pp 3231-3238.

[4] Georgy S., Nanometric Tungsten Carbide and Other Steel Hardening Materials. Department of Materials Engineering, Ben-Gurion University of The Negev.

[5] Jia K.; Fischer T. E.; and Gallois B.. Microstructure, Hardness and Toughness of Nanostructured and Conventional WC-Co Composites. *Nanostructured Materials*, **1998,** 10, pp 875-891.

[6] Inframat Corporation Web Page. http://http://www.inframat.com/wcdetail.htm (accessed July 1, 2015).

[7] Lockwood G. et al. Impregnated Diamond Cutting Structures. U.S. Patent 7,350,599 B2. April 01, 2008.

[8] Artini C.; Muolo M. L.; and Passerone A. Diamond-Metal Interfaces in Cutting Tools: A Review. *J Mater Sci*. **2011,** 47, pp 3252-3264.

[9] Jia K.; Fischer T. E.; and Gallois B.. Microstructure, Hardness and Toughness of Nanostructured and Conventional WC-Co Composites. *Nanostructured Materials*. **1998,** 10, pp 875-891.

[10] Wang X.; Hwang K. S.; Koopman M.; Fang Z.; and Zhang L.. Mechanical Properties and Wear Resistance of Functionally Graded WC-Co. *Intl. J., Refractory Metals and Hard Matls*. **2013,** 36, pp 46-51.

[11] Archimedes' Principle. *Wikipedia* [Online]; Unknown writer, Last Modified September 16, 2015. https://en.wikipedia.org/wiki/Archimedes'_principle (accessed September 17, 2015).

[12] Gordon England Co. Web Page. http://www.gordonengland.co.uk/hardness/vickers.htm (accessed June 16, 2015).

[13] Patil S.. University of Alaska Fairbanks, Fairbanks, AK. Personal communication, 2009.

[14] Metallographic Phase Quantitative Analysis. Baidu Inc. [Online]; Jing Gao & gwy_007, Posted March 21, 2011. http://wenku.baidu.com/view/94a6bd72f242336c1eb95e95.html (accessed June 20. 2015).

[15] Kingland Web Page. http://www.kinglandglobal.com/products/3000hp-drilling-rig/ (accessed June 20, 2015).

[16] Haines, J.; Leger J.M.; and Bocquillon G.. Synthesis and Design of Superhard Materials. *Annual Review of Materials Research*. **2001,** 31, pp 1-23.

[17] Hampshire, S.. Fundamental Aspects of Hard Ceramics. In *Comprehensive Hard Materials*; Elsevier Ltd.: New York, 2014; pp 3-28.

[18] Brookes, K. J. A.. *Hardmetals and Other Hard Materials*; International Carbide Data: London, 1992; pp 1-220.

[19] Prakash, L.. Fundamentals and General Applications of Hardmetals. In *Comprehensive Hard Materials*; Elsevier Ltd.: New York, 2014; pp 29-90.

[20] Konyashin, I.. Cemented Carbides for Mining, Construction and Wear Parts. In *Comprehensive Hard Materials*; Elsevier Ltd.: New York, 2014; pp 425-452.

[21] Fang, Z. Zak; Koopman Mark C.; and Wang Hongtao. Cemented Tungsten Carbide Hard Metal-An Introduction. In *Comprehensive Hard Materials*; Elsevier Ltd.: New York, 2014, pp 123-137.

[22] Frandsen, Marvin V.; and Williams Wendell S.. Thermal Conductivity and Electrical Resistivity of Cemented Transition-Metal Carbides at Low Temperatures. *Journal of the American Ceramic Society*. **1991,** 74, pp 1411-416.

[23] Chandler, H.. *Introduction to Hardness Testing*; ASM Int.: Materials Park, 1999; 2nd Ed., pp 1-14.

[24] Petroleum Services Association of Canada (PSAC) Web Page. http://www.psac.ca/wp-content/uploads/wcs_sample.pdf (accessed June 20, 2015).

[25] Sun, M.. *Zuanjing Wanjing Gongcheng Jichu Zhishi Shouce*: Petroleum Industry Press: Beijing, 2002; pp 2-99.

[26] Materials Modification Inc. Web Page. http://www.matmod.com/publications/armor_1.pdf (accessed July 18, 2015).

[27] Santhanam A. T.; Tierney P.; and Hunt J. L.. *Cemented Carbides*; ASM Int.: Materials Park, 1990; Vol. 2, 10th Ed., pp 950-977.

[28] Properties of Diamond. De Beers Industrial Diamond Division, Special publication K4000/5/89, 1989.

[29] *Product Information Brochure EV-2003*. EPSI isostatic press. Engineered Pressure Systems Incorporated: Haverhill, 2003; pp 2-3.

[30] Hughes, F. H.. The Early History of Diamond Tools. *Industrial Diamond Review*. **1980,** 40, pp 405–407.

[31] Hughes, F. H.. *Diamond Grinding of Metals*. Industrial Diamond Information Bureau: Ascot, U.K., 1978; pp 1–3.

[32] Tolansky, S.. *Early Historical Uses of Diamond Tools*. In Proceedings of the International Industrial Diamond Conference 'Science and Technology of Industrial Diamonds,' edited by Burls, J., Vol. 2, Industrial Diamond Information Bureau: London, 1967, pp 341–349.

[33] Jones, W. D.. *Fundamental Principles of Powder Metallurgy*. Edward Arnold Publishers Ltd.: London, 1960; pp 807.

[34] Jennings, M.. And the Next 50 Years? *Industrial Diamond Review*. **2003,** 63, pp 15.

[35] Baert, M.. *Coating of Diamonds and Granulation of Metal Powders*. In Proceedings of Seminar on PM Diamond Tools, Lausanne, Switzerland, November 2–3, 1995, pp 24–40.

[36] Van Doorslaer, T.. *Coating of Abrasive Grains and the Granulation of Metal Powders*. In Proceedings of International Workshop on Diamond Tool Production, Turin, Italy, November 8–10, 1999, pp 83–88.

[37] Burckhardt, S.. New Technique for Granulating Diamond and Metal Powders. *Industrial Diamond Review*. **1997,** 57, pp 121–122.

[38] Kimura, K.. Method for Forming Metal-coated Abrasive Grain Granules. U.S. Patent 4,770,907, September 13, 1988.

[39] Konstanty J.. *Powder Metallurgy Diamond Tools*; Elsevier: Amsterdam, 2005; pp 76.

[40] Cleavage (crystal). *Wikipedia* [Online]; Unknown writer, Posted April 29, 2015. https://en.wikipedia.org/wiki/Cleavage_(crystal) (accessed August 8, 2015).

[41] Gauthier, E.. Diamond Lap. U.S. Patent 1,625,463, April 19, 1927.

[42] Environment & Energy Publishing, LLC. Web Page. http://www.eenews.net/stories/1059989393 (accessed June 12, 2015).

[43] Lockwood G. T.; Oldham T. W.; Griffo A.; Keshavan M. K.; and Conroy D. A.. Method of Forming Impregnated Diamond Cutting Structures. U.S. Patent 7,845,059 B2. December 07, 2010.

[44] Ding, Huadong; Li Yawen; Yang Xiaohua; Hao Hongqi; and Jin Zhihao. Design of a Non-homogeneous Diamond Bit Matrix. *Journal of Materials Processing Technology*. **1998,** Vol. 84, Issues 1-3, pp 159-161.

[45] Karagőz Ş.; and Zeren M.. Sintering of Polycrystalline Diamond Cutting Tools. *Mater. & Des*. **2007,** 28, pp 1055-1058.

[46] Karagőz Ş.; and Zeren M.. The Property Optimization of Diamond-cutting Tools with the Help of Microstructural Characterization. *Int. J., Refract. Met. Hard Mater*. **2001,** 19, pp 23-26.

[47] Lin C.S.; Yang Y. L.; and Lin S. T.. Performance of Metal-bond Diamond Tools in Grinding Alumina. *J. Mater. Process Technol*. **2008,** 201, pp 612-617.

[48] Xu X.; Tie X. R.; and Wu H.. The Effects of a Ti Coating on the Performance of Metal-bonded Diamond Composites Coating Rare Earth. *Int. J., Refract. Met. Hard Mater*. **2007,** 25, pp 244-249.

[49] Spriano S.; Chen Q.; Settineri L.; and Bugliosi S.. Low Content and Free Cobalt Matrices for Diamond Tools. *Wear*. **2005,** 259, pp 1190-1196.

[50] A Review of Diamond and CBN Sizing & Standards. *Industrial Diamond Association of America, Inc*. Publication No. S&S593 5M.

[51] Bjerregaard, L.; Geels, K.; Ottesen, B.; and Rűckert, M.. *Metalog Guide*. Struers Tech. A/S: Rødovre, Denmark, 1992; pp 5-684.

[52] Prekwinkel, H.. Single-crystal Diamond Tools for Laminated Floors. *Industrial Diamond Review*. **1997,** 57, pp 44-46.

[53] Herbert, S. A.. *Micron Diamond - an Advancing Technology*. Daniel, P., Eds.; De Beers Industrial Diamond Division: Ascot, 1983; Vol. 2, pp 112-125.

[54] Walmsley, J. C.; and Lang, A.R.. *TEM Study of SYNDAX3, Compared with SYNDITE and AMBORITE*. Barrett, C. Eds.; De Beers Industrial Diamond Division: Ascot, 1988; Vol. 4, pp 61–75.

[55] Tomlinson, P.N.; and Clark, I.E.. SYNDAX3 Pins – New Concepts in PCD Drilling. *Industrial Diamond Review*. **1992,** 52, pp 109–114.

[56] Ersoy, A.; and Waller, M. D.. Drilling Detritus and Operating Parameters of Thermally Stable PCD Core Bits. *International Journal of Rock Mechanics and Mining Sciences*. **1997,** 34, pp 1109–1123.

[57] Tillmann, W.. Trends and Market Perspectives for Diamond Tools in the Construction Industry. *International Journal of Refractory Metals & Hard Materials*. **2000,** 18, pp 301–306.

[58] Clark, I. E.; and Sen, P. K.. Advances in the Development of Ultrahard Cutting Tool Materials. *Industrial Diamond Review*. **1998,** 58, pp 40–44.

[59] Derjaguin, B. V.; and Fedoseev, D. V.. Low Pressure Diamond Growth. *Industrial Diamond Review*. **1990,** 50, pp 155–160.

[60] Cooley, B. A.; and Juchem, H. O.. *Vitrified Bonds - No Longer a Synonym for Conventional Abrasive Tools*. In Proceedings of Superabrasives' 85, Chicago, U.S.A., April 22–25, 1985, pp 2.15–2.56.

[61] Bailey, M. W.; and Juchem, H. O.. Selection and Use of Premadia. *Industrial Diamond Review*. **1994,** 54, pp 8–11.

[62] Bakoń, A.; and Szymański, A.. *Practical Uses of Diamonds*. Ellis Horwood: Hemel Hempstead, Herts, U.K. & Polish Scientific Publishers: Warszawa, 1993; pp 124–130.

[63] Jennings, M.. Special Tooling for Specialist Tools. *Industrial Diamond Review*. **1998,** 59, pp 6–7.

[64] Bailey, M. W.; Garrard, R.; and Juchem, H. O.. Characteristics of Diamond and Their Effect on Grinding Behaviour. *Industrial Diamond Review*. **1999,** 59, pp 10–19.

[65] von Mackensen, V.; Longerich, W.; Dennis, P.; and Preising, D.. Fine Grinding with Diamond and cBN. *Industrial Diamond Review*. **1997,** 57, pp 40–43.

[66] Schwan, G.; and Zimmerer, R.. Economic Polishing of Granite. *Industrial Diamond Review*. **1998,** 58, pp 4–5.

[67] Anon., Syndie & Monodie - the Largest Die Blank Range in the World. *Industrial Diamond Review*. **1991,** 51, pp 168–172.

[68] Clark, I. E.; and Sen, P. K.. Advances in the Development of Ultrahard Cutting Tool Materials. *Industrial Diamond Review*. **1998,** 58, pp 40–44.

[69] Cook, M. W.. Diamond Machining of MMC Engineering Components. *Industrial Diamond Review*. **1998,** 58, pp 15–18.

[70] Clark, I. E.. PCD Wood Tools - a New Design Concept. *Industrial Diamond Review*. **1993,** 53, pp 73–76.

[71] Feenstra, R.. Status of Polycrystalline-diamond-compact Bits: Part 1 - Development. *Journal of Petroleum Technology*. **1988,** 40, pp 675–684.

[72] Elsevier Web Page. http://www.journals.elsevier.com/international-journal-of-refractory-metals-and-hard-materials/ (accessed May 20, 2015).

[73] Artini, C.; Muolo M. L.; and Passerone A.. Diamond–metal Interfaces in Cutting Tools: A Review. *J Mater Sci Journal of Materials Science*. **2011,** 47, pp 3252-3264.

[74] Jennings, M.; and Wright, D.. Guidelines for Sawing Stone. *Industrial Diamond Review*. **1989,** 49, pp 70–75.